

ALPINE ARCHITECTURE AND KINEMATICS OF DEFORMATION OF THE NORTHERN PELAGONIAN NAPPE PILE IN THE HELLENIDES

Adamantios KILIAS^{1*)}, Wolfgang FRISCH²⁾, Asterios AVGERINAS¹⁾, Istvan DUNKL³⁾, George FALALAKIS¹⁾ & Hans-Jürgen GAWLICK⁴⁾

¹⁾ Department of Geology and Paleontology, University of Thessaloniki, GR-54124, Thessaloniki, Greece;

²⁾ Institute of Geosciences, University of Tuebingen, D-72076, Tuebingen, Germany;

³⁾ Sedimentology and Environmental Geology Geoscience center, University of Goettingen, D-37077, Goettingen, Germany;

⁴⁾ Department for Applied Geosciences and Geophysics, University of Leoben, A-8700, Leoben, Austria;

* Corresponding author, kilias@geo.auth.gr

KEYWORDS

Vardar/Axios Zone
Pelagonian nappe
compression
Hellenides
extension

ABSTRACT

Geological mapping and detailed structural investigations combined with geochronological and stratigraphic data, as well as fission-track age dating carried out on the northern part of the Pelagonian basement and the adjacent Vardar/Axios sedimentary and metamorphic sequences in the Hellenic Alps (northwestern Greece and Former Yugoslavian Republic of Macedonia) allow us to reconstruct the geometry, kinematics and deformation history of the Pelagonian nappe pile during the Alpine orogeny. We distinguish seven deformational events (D_{HP} and D_1 to D_6). Deformation started in Middle to Late Jurassic time and was associated with inneroceanic thrusting, ophiolite obduction, and NW- to WNW-directed nappe stacking of the Lower and Upper Pelagonian unit (D_1). The lower unit was metamorphosed under greenschist to amphibolite facies conditions with relatively high pressures ($T=450-620^\circ\text{C}$, $P=8-12,5\text{ kb}$). Blueschist-facies metamorphic assemblages (D_{HP} , $T=450-500^\circ\text{C}$, $P>12,5\text{ kb}$) are restricted to the boundary zone between both Pelagonian units. Transgressive Late Jurassic to Early Cretaceous shallow-water limestones and clastic sediments on top of the obducted ophiolites are probably related to extension and basin formation simultaneously with nappe stacking and metamorphism in the Pelagonian nappes beneath. Contractual tectonics with the same kinematics as during D_1 continued in Aptian-Albian time and was associated with intense retrogression (D_2 , $T=280-380^\circ\text{C}$, $P=4-5\text{ kb}$). Low-angle mylonitic extensional shear zones of low-grade metamorphism with top-to-NE sense of movement (D_3) developed simultaneously with basin formation and sedimentation of shallow-water limestones and flysch-like sediments in Late Cretaceous to Paleocene times. Intense imbrication under semi-ductile to brittle conditions of all tectonic units occurred during Paleocene to Eocene time with SW-directed movement towards the foreland (D_4). A large Pelagonian antiformal structure formed during D_4 shortening. In Oligocene to recent time, D_5 and D_6 created brittle low- and high-angle normal faults, respectively.

Im nördlichen Teil des Pelagonischen Kristallins und in den metamorphen und sedimentären Gesteinsfolgen der angrenzenden Vardar/Axios-Zone der Helleniden (NW-Griechenland und Frühere Jugoslawische Republik Mazedonien) wurde eine geologische Kartierung und ausführliche strukturgeologische Untersuchungen durchgeführt. Verbunden mit geochronologischen und stratigraphischen Daten erlauben unsere Ergebnisse, die Geometrie, Kinematik und Deformationsgeschichte des pelagonischen Deckenlandes während der alpidischen Gebirgsbildung zu rekonstruieren. Wir haben sieben Deformationsereignisse (D_{HP} und D_1 bis D_6) unterschieden. Die Deformationsgeschichte begann im Mittleren bis Späten Jura mit intra-ozeanischer Überschiebung, Ophiolith-Obduktion und NW- bis WNW-gerichteter Deckenstapelung der Unteren und Oberen Pelagonischen Einheit (D_1). Die untere Einheit wurde unter den Bedingungen der Grünschiefer- bis Amphibolitfazies bei relativ hohem Druck metamorph überprägt ($T\ 450-620^\circ\text{C}$, $P\ 8-12,5\text{ kb}$). Blauschieferfaziale Paragenesen sind in der tektonischen Kontaktzone zwischen den beiden pelagonischen Einheiten erhalten (D_{HP} : $T\ 450-500^\circ\text{C}$, $P\ >12,5\text{ kb}$). Transgressiv auf obduzierten Ophiolithen abgelagerte oberjurassische bis unterkretazische Flachwasserkalke und klastische Sedimente sind wahrscheinlich mit Extension und Beckenbildung im obersten Krustenstockwerk und gleichzeitiger Deckenstapelung und Metamorphose in den unteren pelagonischen Decken verbunden. Im Aptium-Albium setzte sich die Einengungstektonik mit derselben Kinematik wie während D_1 fort und ging mit intensiver retrograder Metamorphose einher (D_2 : $T\ 280-380^\circ\text{C}$, $P\ 4-5\text{ kb}$). Flach einfallende mylonitische Abscherungszonen, die unter schwachen grünschieferfazialen Metamorphosebedingungen NE-gerichteten Schersinn anzeigen (D_3), entwickelten sich während der Oberen Kreide und des Paleozäns, gleichzeitig mit Beckenbildung und Sedimentation von Flachwasserkalken und Flysch. Intensive Verkürzung und Imbrikation aller tektonischen Einheiten (D_4) fand unter semiduktilen bis spröden Bedingungen und nach SW (gegen das Vorland) gerichteter Hauptbewegung während des Paleozäns bis Eozäns statt. Eine große Antiform bildete sich im Pelagonikum während dieser Einengungsphase. Vom Oligozän bis heute bildeten sich spröde, flach oder steil geneigte Abschiebungen (D_5 und D_6).

1. INTRODUCTION

The Hellenides constitute the southeastern part of the Alpine orogenic belt in Europe (Fig. 1). They are traditionally divided into the Internal Hellenides characterized by Mesozoic, Paleo-

zoic and older metamorphic rocks as well as ophiolites, and the External Hellenides mainly built up by Mesozoic and Cenozoic carbonates and flysch. The External Hellenides form a

SW- to SSW-vergent thinskin fold and thrust belt of Palaeogene to Neogene age.

The Internal Hellenides are subdivided into several metamorphic zones, from E to W (Fig. 1; Brunn, 1956; Godfriaux, 1968; Mercier, 1968; Jacobshagen et al., 1978; Jacobshagen, 1986; Mountrakis, 1986; Kiliias, 1991; Smith, 2006; Himmerkus et al., 2006; Anders et al., 2007; Gawlick et al., 2008; Papanikolaou, 2009): Rhodope Massif = allochthonous terrane, Serbomacedonian Massif = Europe/Asia, Circum-Rhodope belt = European Mesozoic continental margin sediments, Vardar/Axios Zone = Vardar/Tethys oceanic sequence in between Eurasia and Apulia, Pelagonian nappe system (Pelagonian Zone) = eastern passive margin of Gondwana/Apulia or microcontinent in between two oceanic realms. To the west of the Pelagonian Zone the Mirdita/Pindos ophiolitic belt is located and to the east of it the Vardar/Axios ophiolitic belt. A Paleocene to Eocene internal high-pressure/low-temperature (HP/LT) metamorphic belt is developed along the tectonic contact between External and Internal Hellenides (in Olympos-Ossa area; Godfriaux, 1968; Schermer et al., 1990; Kiliias et al., 1991). A second, external, Oligocene to Miocene HP/LT metamorphic belt

is contained in the External Hellenides (in Peloponnesus and Crete; Seidel et al., 1982).

Alpine orogeny in the eastern Mediterranean area is the result of the convergence and final collision of the Apulian and European plates associated with the closure of the Tethys/Vardar Ocean (Fig. 1). Inneroceanic thrusting in the Tethys Ocean started in late Early Jurassic as reported by Ar/Ar dating of metamorphic soles (around 180-170 Ma Roddick et al., 1979; Spray and Rodding, 1980; Dimo, 1997; Pamic, 2002; Karamata, 2006) and ophiolite obduction over the Pelagonian nappes around the Middle/Late Jurassic boundary (Bernoulli and Laubscher, 1972; Mercier et al., 1975; Zimmerman and Ross, 1976; Jacobshagen et al., 1978; Vergely, 1984; Robertson et al., 1996; Rassios and Moores, 2006; Karamata, 2006; Gawlick et al., 2008; Schmid et al., 2008). The internal, structurally higher nappes including parts of the Pelagonian nappe system record the Middle to Late Jurassic stages of deformation. During Late Cretaceous and Tertiary time deformation successively affected the tectonically lower and more external nappes associated with the emplacement of the Pelagonian nappes onto the external units (Fig. 1,2).

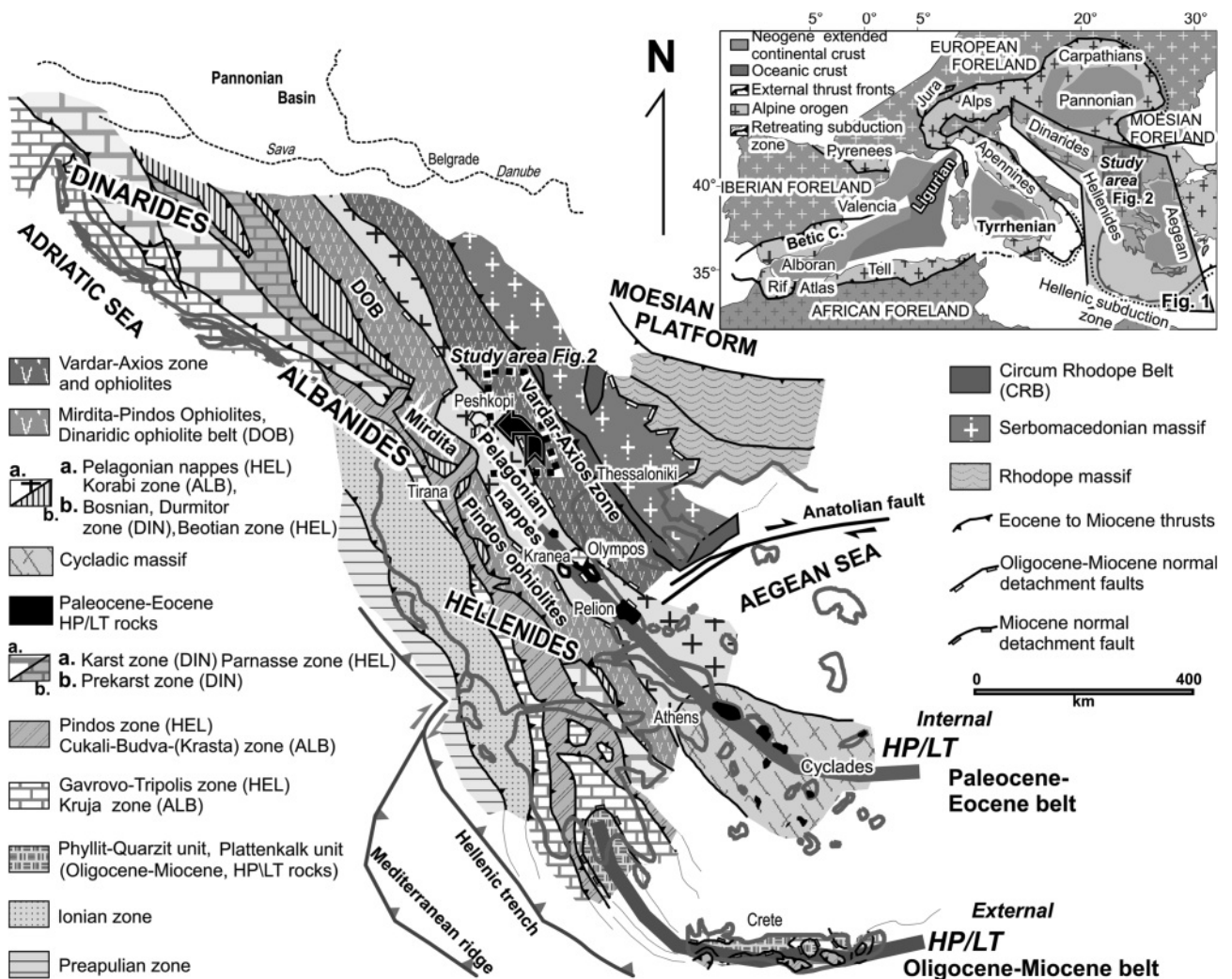


FIGURE 1: Main structural domains of Dinarides and Hellenides with study area in the box (Fig. 2). Modified after Kiliias et al. (2002). Insert: Alpine orogenic belt and Tertiary extensional basins in the Mediterranean region. Modified after Platt et al. (1998).

Late Cretaceous to Tertiary nappe stacking and crustal thickening were followed by orogenic collapse causing extensional structures, crustal thinning, and exhumation of deeper tectonic

units (Godfriaux, 1968; Burchfiel, 1980; Jacobshagen et al., 1978; Lister et al., 1984; Kiliyas and Mountrakis, 1987; Schermer et al., 1990; Sfeikos et al., 1991; Schermer, 1993; Lips et

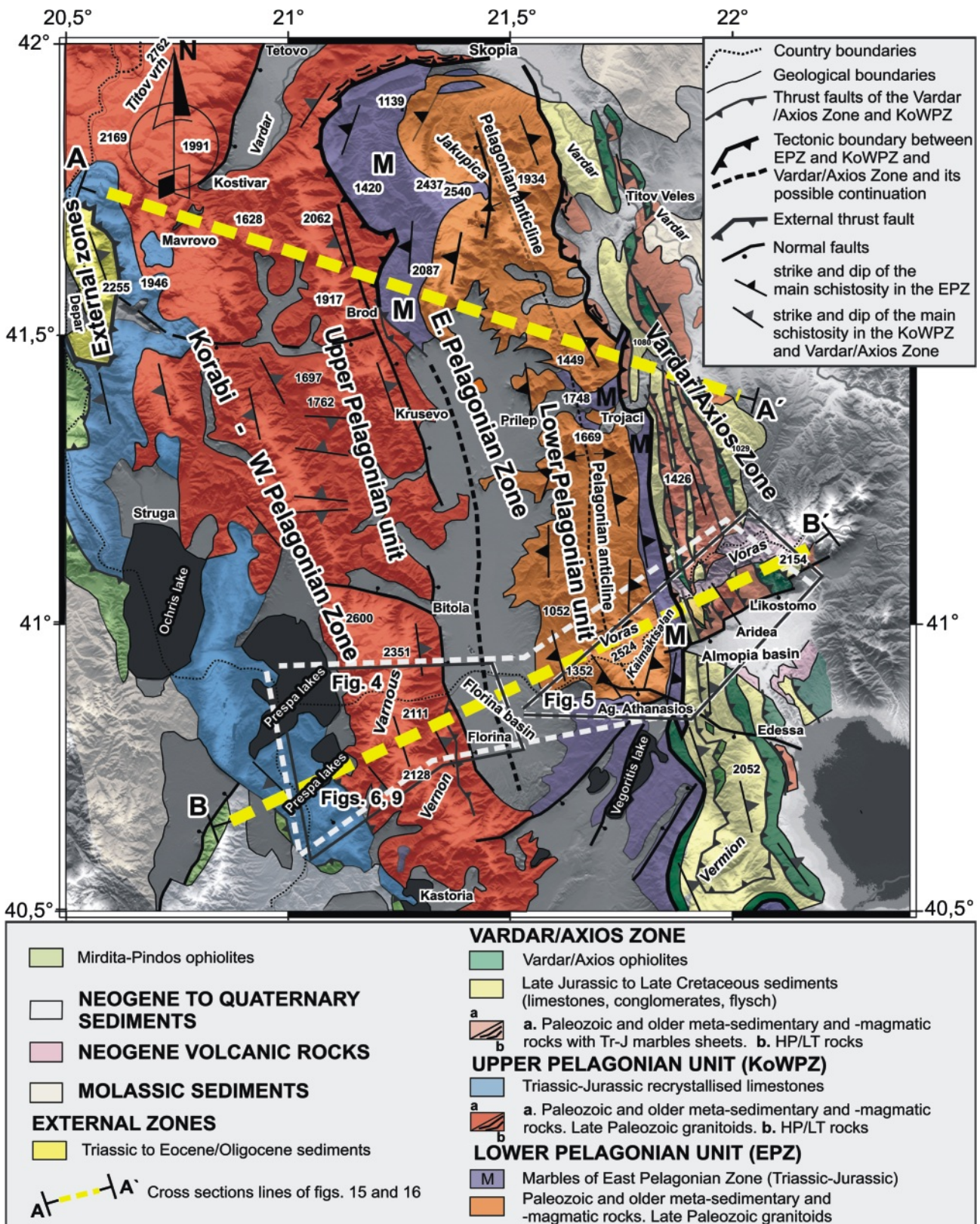


FIGURE 2: Geological map of northern Pelagonian nappes and Vardar/Axios Zone (modified after Medwenitsch, 1956; Dumurzdanov et al., 1976; Mountrakis, 1986; Kiliyas, 1991; Brown and Robertson, 2004). The area of the small boxes is shown in Fig. 4, 5 that of the large box is enlarged in Fig. 6, 9. A-A', B-B' cross-section lines of Fig. 11.

al., 1998; Kiliias et al., 2002). While the Tertiary structural evolution of the Hellenides has been studied in detail and is satisfactorily understood (Schermer et al., 1990; Sfeikos et al., 1991; Schermer, 1993; Dinter and Royden, 1993; Fassoulas et al., 1994; Kiliias et al., 1999; Xypolias et al., 2003), the geometry and kinematics of the early stages of the Alpine orogenic cycle in Jurassic and Cretaceous times still remains poorly studied and contradictory. Tertiary deformation in some cases has totally destroyed the older structures.

In order to decipher the deformational processes during the early stages of the Alpine cycle and their migration until Tertiary time, our study focused on the structurally higher units, i. e., the Pelagonian nappes and the Vardar/Axios Zone from the Voras Mountains in northwestern Greece and the Former Yugoslavian Republic of Macedonia (FYROM) (Fig. 1,2). From this area no comprehensive structural study exists, especially from those parts situated in FYROM.

Timing of deformation was constrained by radiometric results mainly derived from Most (2003), stratigraphic data from Brown and Robertson (2004) and Sharp and Robertson (2006), as well as cross-cutting relationships of structures on all scales from map to thin section. P-T metamorphic conditions were estimated using metamorphic mineral assemblages and thermobarometric calculations. Shear criteria such as S-C fabrics, shear bands, asymmetric pressure shadows, mica fish, or asymmetric boudins (Simpson and Schmid, 1983; Lister and

Snoke, 1984) have been used in order to study the kinematic history of deformation.

2. GEOLOGICAL SETTING

The Pelagonian Zone forms an elongate, NNW-SSE trending nappe pile of continental origin extending from FYROM to the south through the central Greek mainland and Evvia into the Cyclades (Attico-Cycladic Massif) (Fig. 1, 2). In Triassic to Jurassic time the palaeogeographic position of Pelagonian Zone is discussed controversially. One group of authors (Mountrakis, 1986; Robertson et al., 1996; Robertson and Shallo, 2000; Stampfli and Borel, 2002; Brown and Robertson, 2004; Sharp and Robertson, 2006; Rassios and Moores, 2006; Karamata, 2006) reconstructs Pelagonian as a continental block that was bordered by two Tethyan oceanic realms. The Mirdita/Pindos Ocean at its western margin and the Vardar/Axios Ocean at its eastern margin. In contrast another group of authors (Mercier et al., 1975; Burchfiel, 1980; Hoxha, 2001; Bortolotti et al., 2005; Gawlick et al. 2008; Schmid et al., 2008) favours a single oceanic basin to the east, the Tethys (Vardar/Axios) Ocean (Fig. 1, 2). In this concept the Pelagonian units formed the eastern passive continental margin of Gondwana/Apulia facing the Neotethys Ocean. There is also an ongoing discussion about the displacement direction of the obducted ophiolites during Middle to Late Jurassic time onto the Pelagonian continent (in present-day coordinates of continental Greece):

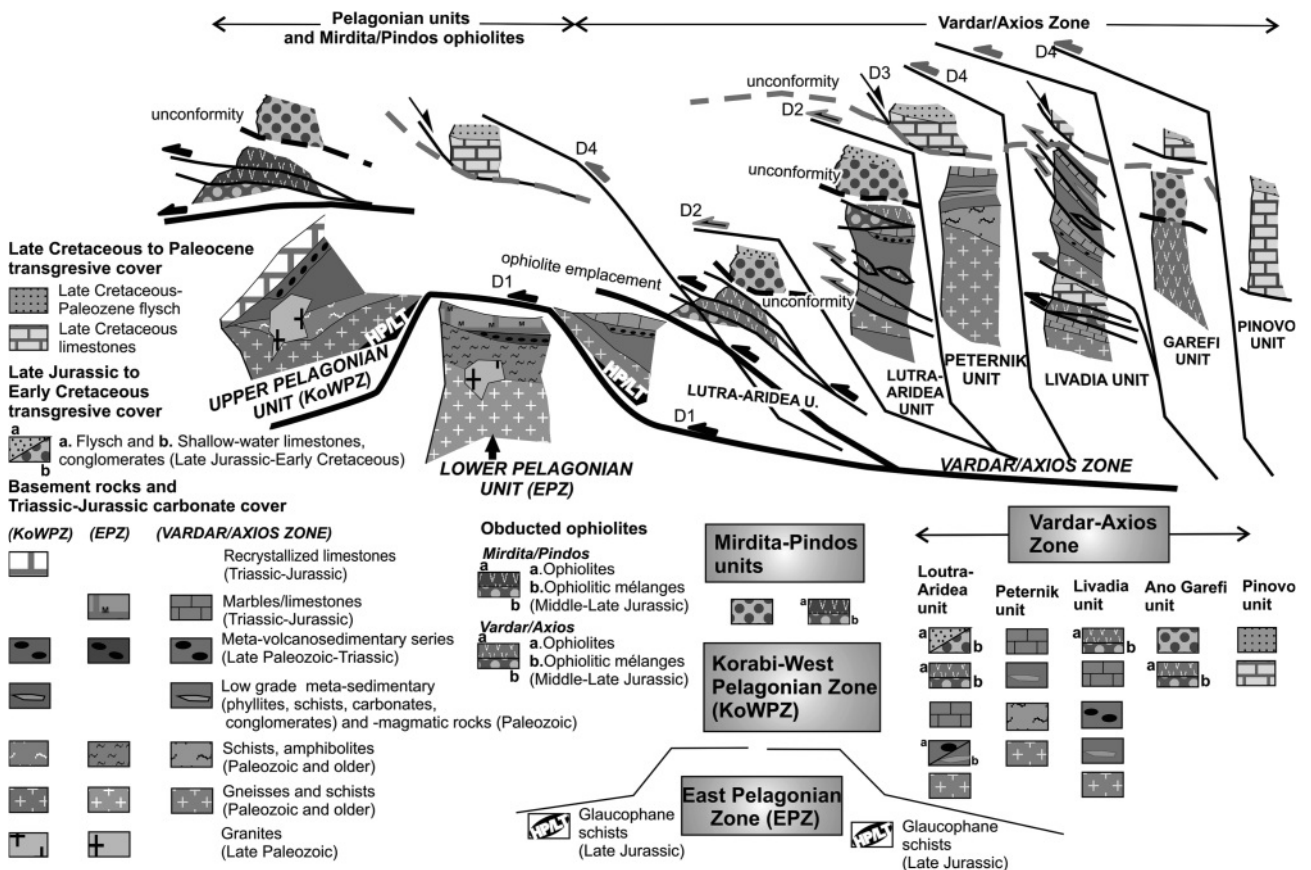


FIGURE 3: Tectonostratigraphy (not to scale) of the imbricated Vardar/Axios units and Pelagonian nappes showing the sequence of deformation (D₁ to D₄) as based on this study and Brown and Robertson (2004).

Time	Area	Northern Pelagonian Zone		Southern Pelagonian Zone			
		KoWPZ (a)	EPZ (b)	Pieria (c)	Olympos (d)	Ossa (e)	Pelion (f)
TERTIARY	Mioc.						
	Olig.						
	Eoc.						
	Pal.						
CRETACEOUS	Late						
	Early						
JURASSIC							

TABLE 1: Main structural and geochronological data from previous works about the Alpine tectonometamorphic events affected the Pelagonian nappe system. Black lines, high pressure event; grey lines, greenschist or amphibolite facies event. Arrows indicate sense of movement. a: Koroneos et al. (1993), b: Most (2003), Borsi et al. (1966), c: Barton (1976), Yarwood and Dixon (1977), d: Schermer et al. (1990), e, f: Lips et al. (1998).

E- to NE-ward direction (e.g. Robertson and Shallo, 2000; Rassios and Dilek, 2009) or W- to SW-ward direction (e.g. Jacobs-hagen et al., 1978; Vergely, 1984; Hoxha, 2001; Gawlick et al., 2008; Schmid et al., 2008 or both e.g. Mountrakis, 1986; Sharp and Robertson 2006).

The structural sequence of the Pelagonian Zone in northern Greece comprises, from top to bottom (Brunn, 1956; Mercier, 1968; Nance, 1981; Mountrakis, 1986; Kiliias and Mountrakis, 1987; Koroneos et al., 1993; Vavassis et al., 2000; Kotopouli

2001). Table I summarises the data of previous structural and geochronological studies about the Alpine tectono-metamorphic events affected the Pelagonian basement. An amphibolite facies metamorphic event during pre-Alpine time (of Variscan age?) is referred to by several authors (e.g. Mountrakis, 1986; Mposkos et al., 2001) but without any exact geochronological analysis.

A different tectono-stratigraphic subdivision is given for the Pelagonian Zone in FYROM, where the Korabi – West Pelagonian Zone (KoWPZ) is distinguished from the East Pelagonian Zone (EPZ) (Medwenitsch, 1956; Arsovski et al., 1977; Dumurdzanov et al. 2005).

The KoWPZ consists of low-grade metamorphosed Ordovician to Late Paleozoic sedimentary and igneous rocks overlain by Triassic-Jurassic carbonates. Schists and gneisses form the lower parts of the KoWPZ (Fig. 3, 4; Arsovski et al., 1977; Mountrakis, 1986; Kiliias and Mountrakis, 1987; Anders et al., 2006, 2007). The EPZ forms a NNW-SSE trending anticlinorium with gneisses and schists derived from Precambrian protoliths and intruded by Late Paleozoic granitoids in its core (Fig. 2; Avgerinas et al., 2001; Anders et al., 2007). A thick section of dolomitic marbles overlies and frames this core and in turn is overlain by the KoWPZ (Fig. 2). The age of the marble sequence was believed to be Riphean to Cambrian by Arsovski et al. (1977) and Arsovski and Dumurdzanov (1984). However, these mar-

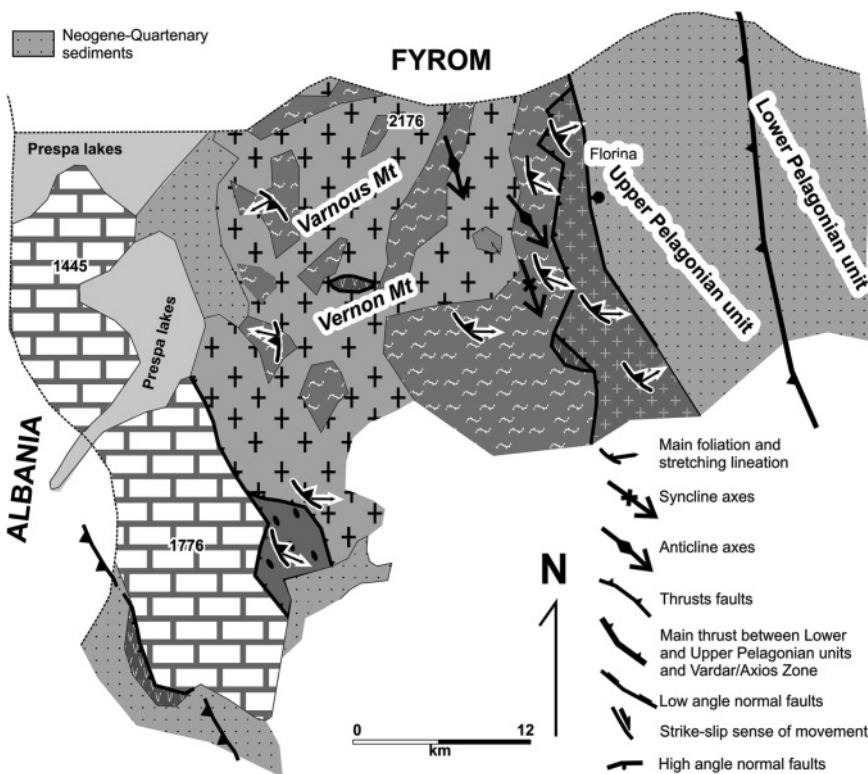


FIGURE 4: Geological and structural map of the Varnous and Vernon Mountains in northwestern Greece. The lowermost units of the KoWPZ and its Permo-Triassic/Jurassic covers with the obducted ophiolites are illustrated. Modified after Mountrakis (1986) and Kiliias (1991). Legend as in Fig. 3.

bles have been dated as Triassic to Early Jurassic in northernmost Greece with *Griphoporella curvata* and Megalodonts (Mercier, 1968; Mountrakis, 1986; Sharp and Robertson, 2006), and as Triassic in FYROM based on $^{87}\text{Sr}/^{86}\text{Sr}$ ratio measurements (Most 2003).

The eastern side of the Pelagonian Zone is truncated by the Vardar/Axios Zone, which is particularly well exposed in the Voras Mountains where the tectono-stratigraphic sequence can be studied best (Fig. 2,3, 5; Mountrakis, 1986; Migros and Galeos, 1990; Galeos et al., 1994; Brown and Robertson, 2004; Sharp and Robertson, 2006; Papanikolaou 2009). It contains narrow belts of schists, gneisses, granitoids, Paleozoic and Mesozoic metasedimentary rocks, Tethyan ophiolites and Middle to Late Jurassic radiolaritic-ophiolitic mélanges. The succession on the top of the obducted ophiolites consists of Late Jurassic to Early Cretaceous clastic sediments and shallow-water limestones and flysch. Transgressive Late Cretaceous neritic limestones unconformably overlie all Vardar/Axios sequences and the Pelagonian marbles. They pass into Maastriichtian to Paleocene flysch. The complicated composition and

structures of the Vardar/Axios units are given in detail in Fig. 3 and 5.

In this paper we regard the East Pelagonian Zone as an exhumed Pelagonian dome (Lower Pelagonian unit) beneath the overthrust Korabi – West Pelagonian zone (Upper Pelagonian unit) and the Vardar/Axios units (Fig. 2, 3). The gneisses, granitoids, schists, Paleozoic metamorphic rocks and Triassic-Jurassic carbonates from KoWPZ and Vardar/ Axios Zone occur on both sides of the dome and form equivalent structural sequences of the same tectonic nappe.

3. RESULTS

3.1 DEFORMATION STRUCTURES AND KINEMATICS

The deformation history of the study area is complicated, because successive events interacted making their distinction difficult in several cases. They document the change from ductile conditions in the early stages of deformation to semi-ductile and eventually brittle conditions in the late stages. Shortening and extension alternated.

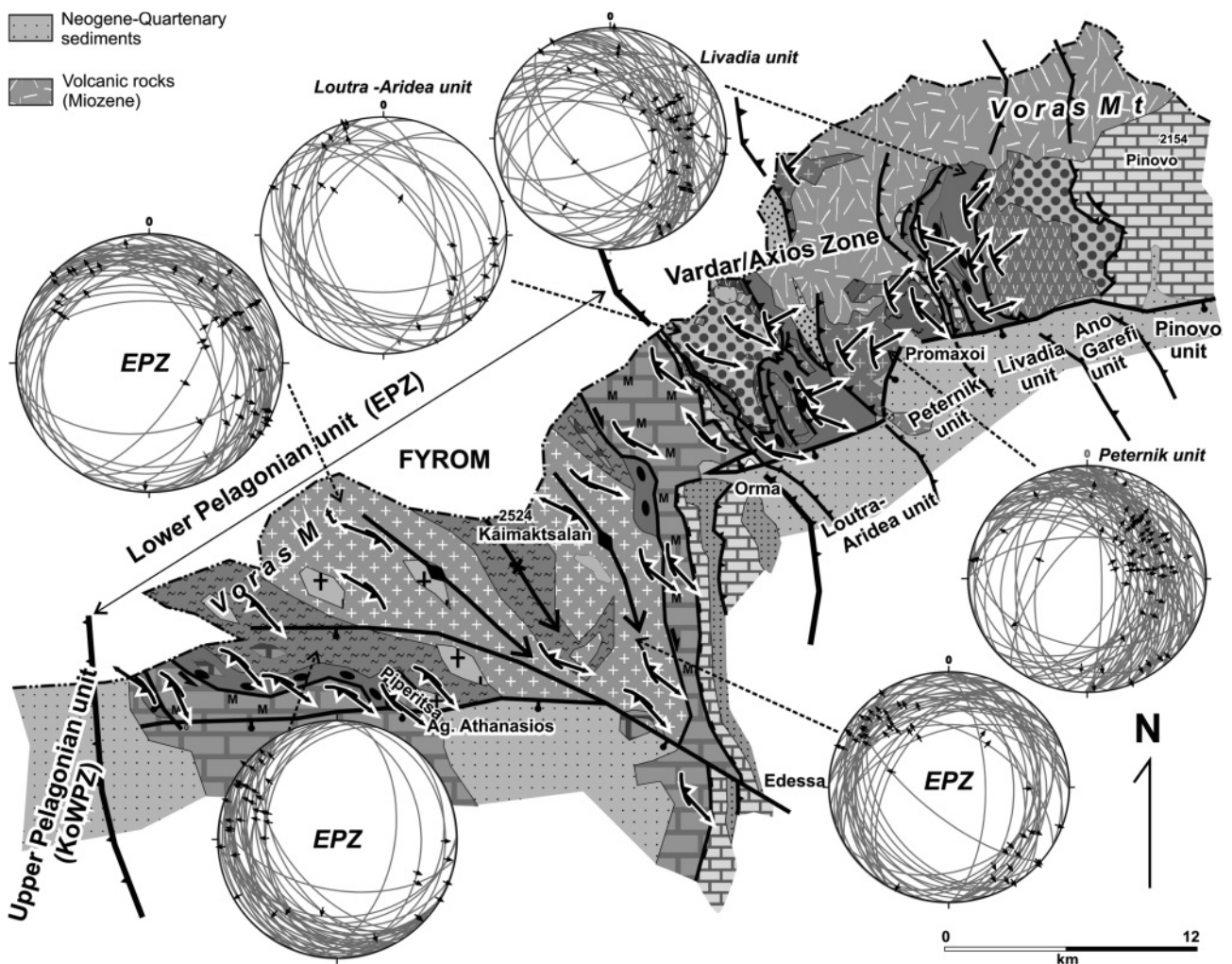


FIGURE 5: Geological and structural map of the Voras Mountains in northwestern Greece based on this study and previous work by Mountrakis (1986), Kiliias (1991), Galeos et al. (1994), Avgerinas et al. (2001). The EPZ metamorphic rocks and the adjacent Vardar/Axios units are illustrated. Schmidt diagrams (lower hemisphere) illustrate the orientation of the main foliation planes (S) and the associated stretching lineations (L) in each tectonic unit. Legend as in Fig. 3 and 4.

The geometry and kinematics of deformation, cross cutting relationships, and the syn-kinematic growth of metamorphic mineral assemblages related to a given structure in combination with regional considerations record the progressive activity of seven (D_{HP} and D_1 to D_6) tectonic events from Middle Jurassic to Neogene time (Fig. 3). They are related to plate convergence and the closure of the Tethyan Ocean, as well as to extensional events like orogenic collapse.

Where possible, fault-slip data were taken in order to calculate the paleostress tensor following the direct stress inversion method (Angelier and Mechler, 1977; Angelier and Goguel, 1979). The solution is considered satisfactory if more than 80 % of the fault-slip data from a site show a misfit angle between the theoretical and real slip vector of less than 30°. The programs My fault, version 1,03 (Pangea scientific, 2005), and Stereo Net (Duyster, 2000) have been used for graphical presentation of the tectonic data.

3.1.1 D_{HP} EVENT

High pressure structures (D_{HP}) are preserved at the boundary between EPZ and KoWPZ and can be traced on top of the marble cover of the EPZ so that it surrounds the East Pelagonian anticlinorium following the tectonic boundary between EPZ and the overlying KoWPZ and Vardar/Axios units, respectively (Fig. 2,3). They are characterized by the occurrence of a relict S_{HP} foliation associated with an about WNW-ESE trending stretching lineation (L_{HP}). L_{HP} is defined mainly by blue amphibole, white mica and chlorite. Majer and Mason (1983) report also sodic pyroxene related to the high pressure event.

3.1.2 D_1 EVENT

The D_1 event records penetrative ductile structures. They are well preserved in the EPZ and along its top tectonic contact. In the KoWPZ and the Vardar/Axios basement no geochronological or stratigraphic data are available to document this event. D_1 created a penetrative syn-metamorphic foliation (S_1) with a general NNW-SSE trend. It dips towards the WSW in the western limb of the EPZ culmination and towards the ENE in the eastern limb (Fig. 5, 6a).

F_1 folds with S_1 as axial plane foliation are scarce. Only small-scale isoclinal folds were observed (Fig. 7a), sometimes also sheath or intrafolial folds with their axis subparallel to L_1 . The L_1 stretching lineation is well developed. Its trend appears not to be constant but mainly NW-SE to WNW-ESE. (Fig. 6a, 8a). Deviations from the main trend is of local importance and are frequently recognized near younger fault zones. A more detailed structural mapping of these faults was outside of our goal in this paper. Chloritoid, white mica, chlorite, K-feldspar and/or plagioclase, garnet, quartz (forming ribbons), staurolite, kyanite, and tschermakitic hornblende are the most common minerals defining S_1/L_1 . Static recrystallisation of quartz created polygonal fabrics and indicate post-kinematic annealing.

The main direction of movement was top-to-WNW or -NW, although divergences from this direction are found in some cases, e.g. towards SE (Fig. 6a, 7b, 8a). NW-directed move-

ment is well documented by S-C fabrics in Paleozoic schists of the Vardar/Axios Zone near Trojaci on the eastern flank of the EPZ (Fig. 7c, d). NE-directed movements on the eastern flank of the EPZ were described by Most et al. (2001), but the age of these structures remained unclear. We consider these structures as belonging to the D_3 event (see below).

3.1.3 D_2 EVENT

The S_1 foliation became affected by asymmetric, overturned to recumbent, narrow to isoclinal folds during the D_2 event (Fig. 7a, a'). The up to kilometre-scale F_2 folds are associated with small-scale S- and Z- type folds. Fold axes are mainly subhorizontal or gently NW- or SE-plunging, although they deviate from this trend in some places.

A pervasive S_2 foliation is axial plane with respect to the F_2 folds and forms the dominant structure of the D_2 event (Fig. 7e, f). It is developed as crenulation cleavage in the hinge zones of the F_2 folds where the otherwise hardly discernible S_1/S_2 relationship becomes clear. Due to transposition of S_1 , the S_1 and S_2 planes are commonly oriented parallel or subparallel to each other. Again, the S_2 foliation dips to the SW and NE at the western and eastern limbs of the EPZ, respectively. This geometry of both the S_1 and S_2 fabrics defines the dome structure of the EPZ (Fig. 6a, 8b).

S_2 is associated with an L_2 stretching lineation which is mainly defined by the preferred orientation of quartz, plagioclase (albite/oligoclase), sericite, chlorite, and actinolite. The minerals defining the S_2 foliation differ from the S_1 minerals and thus indicate lower (greenschist-facies) temperatures of formation: white mica is clearly finer grained (sericite), garnet becomes chloritised and the amphibole is an actinolite or actinolitic hornblende. In general, L_2 gently plunges towards the NW or SE, although other trends are also observed especially in the tectonically higher levels of the Vardar/Axios Zone (e. g., Peternik and Livadia units) as well as in the KoWPZ (Fig. 8b). Shear sense indicators display a dominant top-to-NW or -WNW transport direction (Fig. 7 f,g,h). In some cases an opposite (conjugate), top-to-SE sense of movement is observed. Top-to-SW tectonic transport is mainly recognized in the Peternik and Livadia units of the Vardar/Axios Zone (Fig. 6a, 8b).

3.1.4 D_3 EVENT

D_3 structures are characterized by discrete mylonitic shear zones with dynamic recrystallisation of quartz (Fig. 7 i, j). The S_3 mylonitic foliation in general dips to the NE and the associated, well developed L_3 stretching lineation plunges down-dip (Fig. 6b, 8c). Shear sense indicators such as S-C fabrics, mica fish, asymmetric boudins, and pressure shadows around white mica or feldspar porphyroclasts show a constant down-dip (normal) sense of shear (Fig. 7 i,j). Opposite to SW-dipping D_3 mylonitic shear zones with again normal (top-to-SW) sense of shear are observed in few cases. In contrast to the D_1 and D_2 structures, the D_3 structures show constant geometry and kinematics.

The D₃ mylonitic shear zones are very well developed in the Paleozoic sequences of the Vardar/Axios Zone and the KoWPZ and overprint the penetrative D₂ structures.

3.1.5 D₄ EVENT

D₄ is manifested by open to tight NW-SE trending kink folds, as well as discrete semi-ductile to brittle shear zones indica-

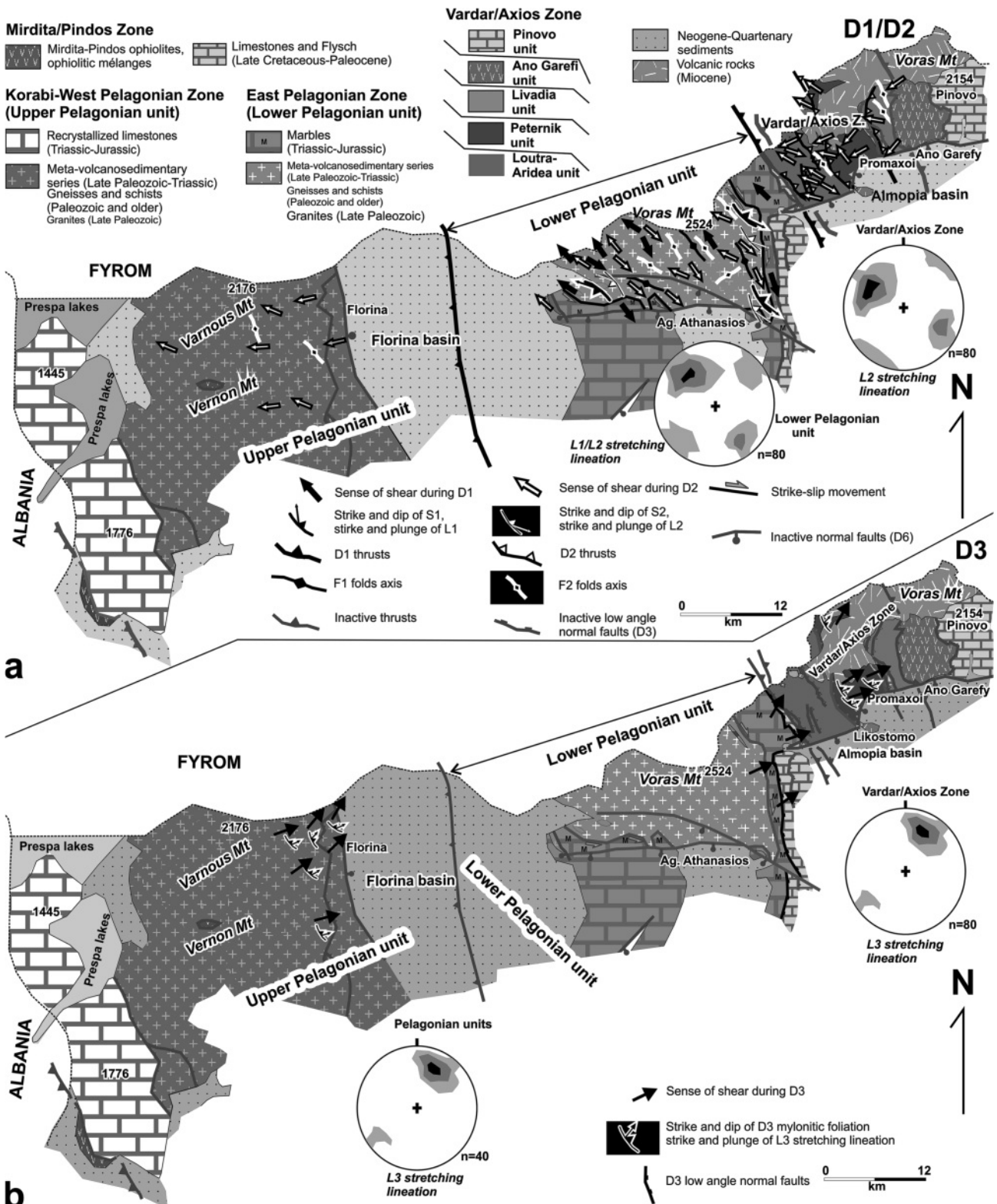


FIGURE 6: Geological and structural maps of the Pelagonian nappes and the Vardar/Axios Zone in northwestern Greece (Varnous, Vernon and Voras Mountains) with the structural elements and the kinematics of the D₁, D₂ (a) and D₃ (b) events. Each symbol represents the mean of 5 to 15 field measurements. Black lines describe the main tectonic contacts during D₁, D₂ (a) and D₃ (b) events, grey lines the main tectonic contacts of the next or previous stages of deformation. Schmidt diagrams (lower hemisphere) show the orientation of the L₁, L₂ (a) and L₃ (b) stretching lineations; contours: 2,5%-5%-7% per 1% area, n=number of measurements.

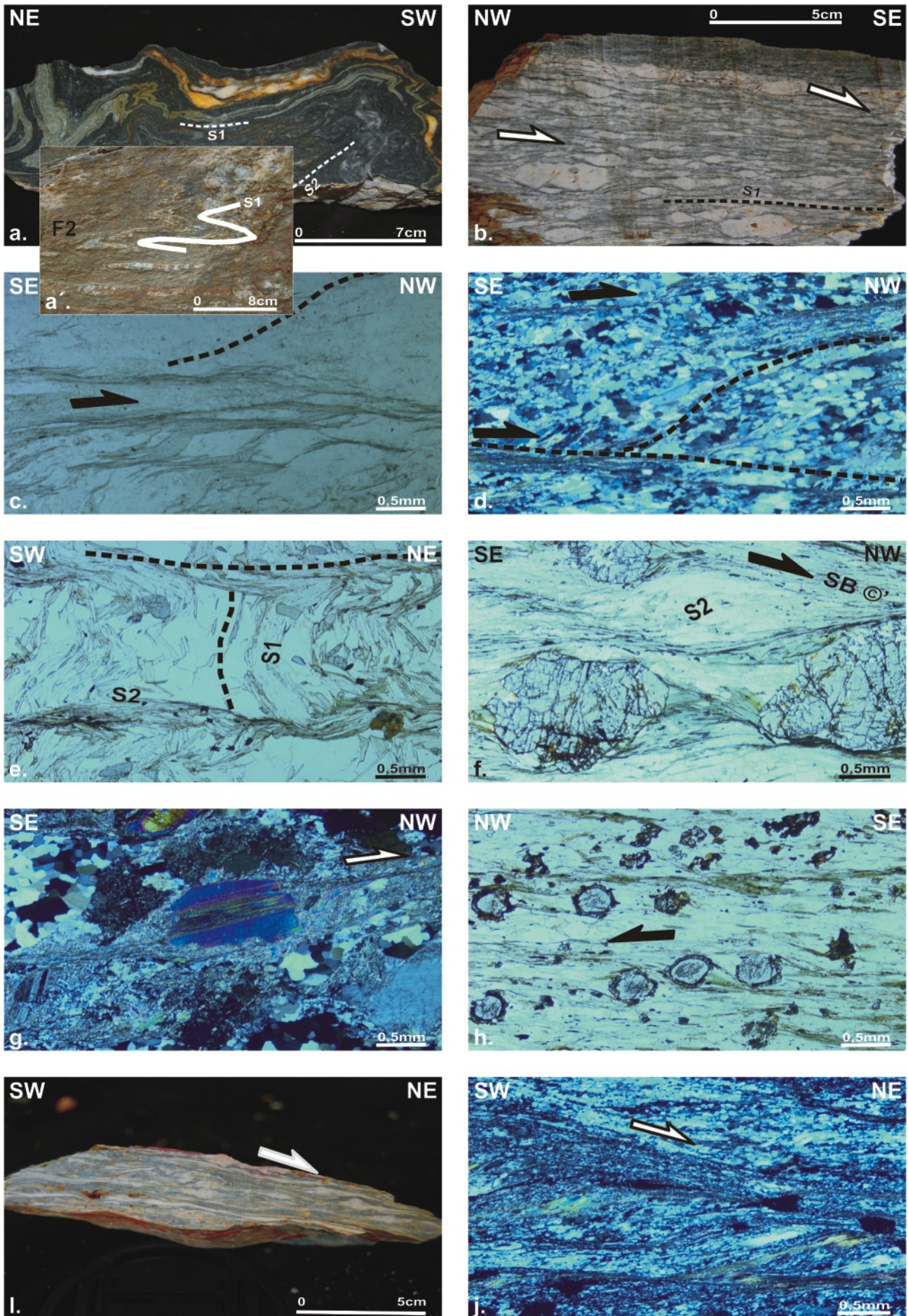


FIGURE 7: Meso- and microscale features of deformation. (a & a') Main S_1 foliation related to F_1 isoclinal folds. Asymmetric F_2 folds overprint F_1 folds. Garnet micaschist (Lower Pelagonian unit). (b) S_1 foliation. Shear bands and feldspar σ -clasts indicate top-to-SE sense of shear. XZ section, arrows indicate sense of shear. White mica augengneiss (Lower Pelagonian unit). (c, d) S-C fabrics in white mica gneiss from tectonic contact between EPZ and Paleozoic schists of Vardar/Axios Zone. XZ section. Sense of shear top-to-NW. (e) S_1/S_2 relationship. S_1 is defined by white mica and chloritoid. Chloritoid rotates into S_2 . YZ section. Garnet-chloritoid micaschist (Lower Pelagonian unit). (f) Shear bands indicating top-to-NW sense of shear during D_2 . Chloritization in pressure shadows of D_1 garnet σ -clasts took place also during D_2 . XZ section. Garnet micaschist (Lower Pelagonian unit). (g) Recrystallization of sericite in S_2 planes around white mica porphyroclast. Asymmetry of mica fish indicates top-to-NW sense of shear. XZ section. Garnet-bearing gneiss of Peternik unit. (h) Garnet with characteristic zonation and internal fabric (S_i) rotated during D_2 . Chlorite aggregates (after garnet) and sericite in asymmetric pressure shadows and along dominating S_2 foliation planes. Garnet σ -clasts and S-C fabric indicate top-to-NW sense of shear. XZ section. Garnet micaschist (Lower Pelagonian unit). (i, j) Augengneisses of the Livadia and Peternik units. Feldspar σ -clasts, S-C fabrics, and shear bands indicate top-to-NE sense of shear (D_3 event). XZ section. Microscopic pictures: c, e, f, h with one nicol, d, g, j with crossed nicols.

ting constant top-to-SW thrusting (Fig. 8d, 9a). F_4 folds are generally SW-vergent, in few cases NE-vergence is observed due to backthrusting during the D_4 event. They fold the D_3 shear zones. Locally the folds are associated with a weakly developed crenulation cleavage without significant recrystallization of quartz. The F_4 fold axes did not experience rotation parallel to the transport direction but are still oriented perpendicular to the direction of thrusting as it is typical of a brittle environment of deformation. A penetrative cleavage is also missing. D_4 occurred at lower temperatures and thus in a more shallow crustal level than the previous events.

D_4 structures are mainly exposed in the Vardar/Axios Zone but also occur in the KoWPZ and the EPZ. Paleostress analyses from D_4 fault populations indicate subvertical σ_3 and subhorizontal, NE-SW trending σ_1 axes (Fig. 9a, 10a).

3.1.6 D_5 EVENT

Brittle low angle shear zones with normal displacement are formed during the D_5 event. They cut all previous structures and juxtapose rocks of higher structural levels against rocks of lower tectonic units. Near Agios Athanasios in the Greek part of the study area the Triassic-Jurassic marbles of the EPZ are directly overlying a Late Paleozoic granite along such a shear zone, cutting out a thick metamorphic sequence of gneisses and schists (Fig. 5, 9b). The northwestern contact between EPZ and KoWPZ in FYROM has been reworked by such D_5 shear zone juxtaposing the low grade metamorphic Paleozoic sequences of the KoWPZ against the marbles of the EPZ cutting out the KoWPZ gneisses and schists (Fig. 2, 11A-A'). Omission of several lithologic units is frequently observed along the entire contact between the EPZ marbles and the underlying units (Fig. 5). However, the complete Permo-Triassic sequence with meta-rhyolitic intercalations is also preserved in some places (Fig. 3, 5).

D_5 shear zones are best recognized in granites and orthogneisses of the Pelagonian nappes as well as in the Vardar/Axios Zone. They are characterized by ultracataclastic rocks. The narrow and discrete shear zones mostly dip towards the SW. Sense of shear is generally downdip. In some cases a strike-slip sense of displacement is observed (Fig. 9b). Fault plane analyses yielded subvertical σ_1 and subhorizontal, SW-NE trending σ_3 axes (Fig.9b, 10b).

3.1.7 D_6 EVENT

D_6 structures overprint all older structures and represent the final deformational stage of the orogen. They are high-angle dip-slip to oblique-slip normal as well as strike-slip faults related to the Neogene-Quaternary basin formation in the study area (Fig. 2, 4, 5, 9b).

Many of the D_6 faults produce significant tectonostratigraphic gaps juxtaposing higher tectonic units against lower ones. As an example, the E-W to ESE-WNW trending high-angle nor-

Sample minerals	8						3						6			22 (Most, 2003)			
	gr	C	chl	chld	wm	R	gr	C	chl	chld	wm	rut	gr	chld	wm	bi	gr	wm	
SiO ₂	38.07	39.93	26.36	25.63	49.15	47.92	38.43	38.18	25.60	24.22	52.37	48.63	0.00	38.82	24.33	49.24	39.35	37.74	49.64
TiO ₂	0.00	0.00	0.00	0.00	0.00	0.00	0.00	0.00	0.00	0.00	0.00	0.58	99.32	0.00	0.00	0.00	0.78	0.00	0.36
Al ₂ O ₃	21.20	20.02	21.2	39.79	30.13	32.99	20.30	20.34	20.84	40.09	29.29	33.72	0	19.56	40.63	33.55	17.99	21.47	33.64
Cr ₂ O ₃	0.00	0.00	0.00	0.00	0.00	0.00	0.00	0.00	0.00	0.00	0.00	0.00	0.00	0.00	0.00	0.00	0.00	0.00	0.00
FeO	30.80	29.71	24.98	21.40	3.06	2.60	32.19	31.07	27.36	24.03	2.09	1.50	1.02	33.80	23.22	1.53	14.70	30.34	1.40
MnO	2.80	3.00	0.00	0.00	0.00	0.00	2.51	3.49	0.00	0.00	0.00	0.00	0.00	5.29	0.00	0.00	0.02	2.73	0.00
MgO	3.42	2.86	14.87	3.77	2.06	1.38	2.15	1.29	13.03	2.60	2.00	1.12	0.00	1.72	2.73	1.10	13.69	4.33	2.19
CaO	4.14	5.16	0.00	0.00	0.00	0.00	3.83	5.35	0.00	0.00	0.00	0.00	0.00	1.03	0.00	0.00	0.00	3.28	0.02
Na ₂ O	0.00	0.00	0.00	0.00	0.76	0.93	0.00	0.00	0.00	0.00	0.69	1.36	0.00	0.00	0.00	1.12	0.29	0.00	1.46
K ₂ O	0.00	0.00	0.00	0.00	9.80	9.59	0.00	0.00	0.00	0.00	10.37	9.40	0.00	0.00	0.00	9.10	8.46	0.00	8.94
Total	100.43	100.75	87.42	90.80	94.96	95.41	99.41	99.73	86.82	90.93	96.76	96.31	100.34	100.22	90.91	95.63	95.62	99.89	97.66
Si					3.293	3.187					3.420	3.184				3.232			3.20
Alm	0.682	0.651					0.735	0.704						0.764					
Sps	0.063	0.072					0.060	0.082						0.130					
Pyr	0.136	0.121					0.090	0.054						0.074					
Grs	0.111	0.077					0.084	0.130						0.048					
Anr	0.008	0.079					0.032	0.030						0.080					
Uvr	0.000	0.000					0.000	0.000						0.000					
Mg/(Mg+Fe)	0.165	0.146					0.107	0.069						0.088					

TABLE 2: Representative electron microprobe analyses of syn- D_1 mineral phases. C, core; R, rim. Samples 8, 3, 6: garnet-white mica-chloritoid schists; 22: garnet-staurolite-kyanite-micaschist. Lower Pelagonian unit.

mal faults along the southern edge of the EPZ schists and gneisses separate their marble cover from the overlying Late Cretaceous to Paleocene limestones and flysch (Fig. 5, 9b).

Some of the D_6 faults show recent activity, often associated with impressive fault escarpments as, e. g., the ca. ENE-WSW trending fault along the northern margin of the Almo-pias basin (Fig. 9b; Pavlides et al., 1990).

3.2 RELATIONSHIPS BETWEEN DEFORMATION AND METAMORPHISM

For the main ductile deformational events (D_{HP} , D_1 and D_2) the P-T metamorphic conditions were calculated from mineral assemblages with syn-kinematic growth with respect to these tectonometamorphic events. Syn-kinematic growth of minerals is indicated by their alignment parallel to the foliation planes

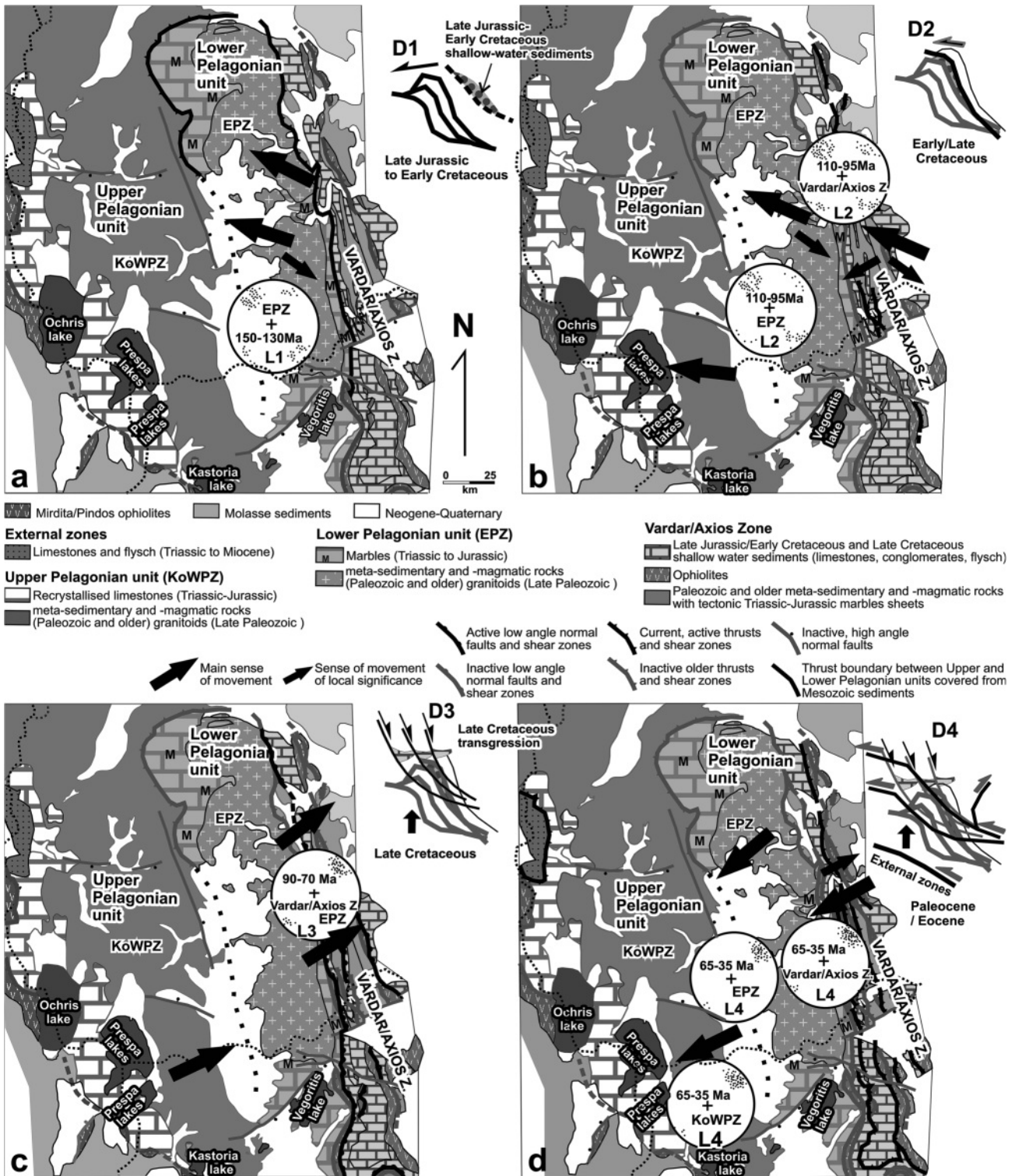


FIGURE 8: Tectonic sketch maps of northern Pelagonian nappes and adjacent Vardar/Axios Zone including major structural elements and sense of movement (arrows) during D_1 (a), D_2 (b), D_3 (c) and D_4 (d) tectonic events.

and the stretching lineation, by sigmoidal internal foliation in rotated plagioclase or garnet and its continuity with the matrix foliation, as well as by the dynamic recrystallisation of quartz along the foliation planes. Syn-kinematic growth of garnet is indicated when the external foliation is deflected around the porphyroblasts, whereas in other cases it is overgrown and preserved within the garnet porphyroblasts.

Metamorphic conditions were calculated with the Tweeq method (Bermann, 1991), the garnet-biotite (Ferry and Spear, 1978), the garnet-muscovite (Hynes and Forest, 1988; Wu et al. 2002), the garnet-chlorite (Grambling, 1990), the muscovite-paragonite (Blencoe et al., 1994), the chloritoid-chlorite (Vidal et al., 1999), and the chlorite (Zang and Fyfe, 1995; Xie et al. 1997) geothermometers, and the phengite component geoba-

3.2.1 HP EVENT

The occurrence of phengite, glaucophane, barroisitic hornblende, and rutile in the amphibolites, gneisses, and schists along the western, northern, and eastern tectonic boundary of the EPZ testifies to the existence of a HP event (Fig. 2, 11).

Oxide	Sample minerals	305			8		85		
		wm	amph	pl	gr	wm	gr	wm	il
SiO ₂		51.54	46.82	68.43	38.01	48.04	39.68	49.03	0.00
TiO ₂		0.00	0.00	0.00	0.00	0.00	0.00	0.00	45.98
Al ₂ O ₃		28.86	13.17	20.93	20.79	32.51	21.58	32.93	0.00
Cr ₂ O ₃		0.00	0.00	0.00	0.00	0.00	0.00	0.00	0.00
FeO		2.90	14.90	0.00	30.82	2.67	32.43	2.97	51.60
MnO		0.00	0.00	0.00	3.24	0.00	0.00	0.00	2.63
MgO		2.11	10.37	0.00	2.30	1.46	3.61	0.00	0.00
CaO		0.00	9.02	0.00	5.34	0.00	3.28	0.00	0.00
Na ₂ O		0.94	2.95	10.85	0.00	1.22	0.00	1.42	0.00
K ₂ O		9.71	0.00	0.00	0.00	9.51	0.00	9.03	0.00
Total		96.05	97.22	100.21	100.50	95.41	100.58	95.39	100.21

TABLE 3: Representative chemical input data for thermobarometric calculation using the Tweeq method. Sample 305: amphibole schist; 8, 85: garnet- white mica-chloritoid schists. Wm white mica, amph amphibole, gr garnet, bi biotite, ilm ilmenite, pl plagioclase.

Method	85 grt-chld-wm schist	305 amph schist	8 grt-chld-wm schist	3 grt-chld-wm schist	16 grt-chld-wm schist	Ka20 grt-chld-wm schist	Ka23 grt-chld-wm schist	Ka25 grt-chld-wm schist
Tweeq	P=12,76±0,04 kbr T=540,61±0,06°C D1	P = 9,63±0,06 kbr T=457,69±0,12°C D1	P=11,60±0,04 kbr T=503,87±0,11°C D1	P=12±0,03 kbr T=480,39±0,07°C D1				
Garnet-Muscovite Wu et al 2002	T=476°-580°C D1		T=510°-543°C D1	T=552°-580°C D1	T=538°-570°C D1	T=520°-585°C D1	T=516°-540°C D1	
Chlorite Cathelineau 1991 Zang & Fyfe 1995 Xie et al. 1997			T=261°-380°C D2	T=242°-340°C D2		T=290°-380°C D2		
Garnet-Chlorite Grambling 1990 Fe ³⁺			T=470°-530° D1	T=464°-530°C D1		T=513°-520°C D1	T=507°-574°C D1	T=506°-580°C D1
Muscovite-Paragonite Blencoe et al. 1994						T=498°-540°C D1	T=465°-504°C D1	
Chloritoid-Chlorite Vidal et al. 1999			T=446°-503°C D1	T=517°-585°C D1		T=560°-580°C D1	T=550°-580°C D1	

TABLE 4: Overview on P-T estimates of samples of the upper tectonostratigraphic levels of the Lower Pelagonian unit.

rometer (Massonne and Schreyer, 1987). Amphibole and biotite compositions were also used to estimate the P-T conditions (Laird et al., 1984; Schreurs 1985).

Mineral chemical analyses were carried out using a JEOV 8900 Superprobe electron microprobe in the Institute of Geosciences of the University of Tübingen. Mineral chemistry of representative phases is given in Table II. Some representative thermodynamic input data for the Tweeq method are presented in Table III. Figure 12 illustrates representative examples of thermobarometric results obtained from the Tweeq program. Tables IV and V show representative results of the P-T estimates.

Method	15. grt-bi-mu schist	24. grt-st-bi-mu schist	22. grt-st-bi-mu schist	10. grt-st-ky schist
Tweeq	P=8±0,16 kb T=530,40±0,01°C D1	P = 12,5±0,08 kb T=595,20±0,15°C D1		
Garnet-Biotite Ferry and Spear (1978) Indares and Martignole (1985)	T = 590-620°C D1	T=586-630°C D1	T=520-630°C D1	T=584-618°C D1
Garnet-Muscovite Wu et al. (2002)	T=580-610°C D1	T=580-630°C D1	T=590-610°C D1	T=597-630°C D1

TABLE 5: Overview on P-T estimates of samples of the lower tectonostratigraphic levels of the Lower Pelagonian unit.

Sodic pyroxene has been found in the boundary zone between EPZ and Vardar/Axios Zone (Majer and Mason, 1983).

Phengitic white mica with maximum 3.5 Si atoms per formula unit (apfu) from a glaucophane schist tectonically above the

EPZ marble cover near Skopje (Fig. 2, 11, 13a) indicates a minimum pressure of 12.5 kb for the D_{HP} (blueschist facies) event (phengite barometer after Massonne and Schreyer, 1987), assuming a temperature of 450-500° C (Most, 2003).

3.2.2 D_1 EVENT

The critical syn- D_1 mineral assemblages of the EPZ domal

structure used for the thermobarometric investigations are as follows. The metapelites are characterized by garnet, white mica, biotite, chlorite, chloritoid, quartz, plagioclase, ilmenite, sphene, kyanite, and epidote. Staurolite appears in the lower structural levels only. Chloritoid and rutile (as a relict HP mineral) are often included in garnet porphyroblasts showing in some cases a well-developed internal foliation. Rutile is often

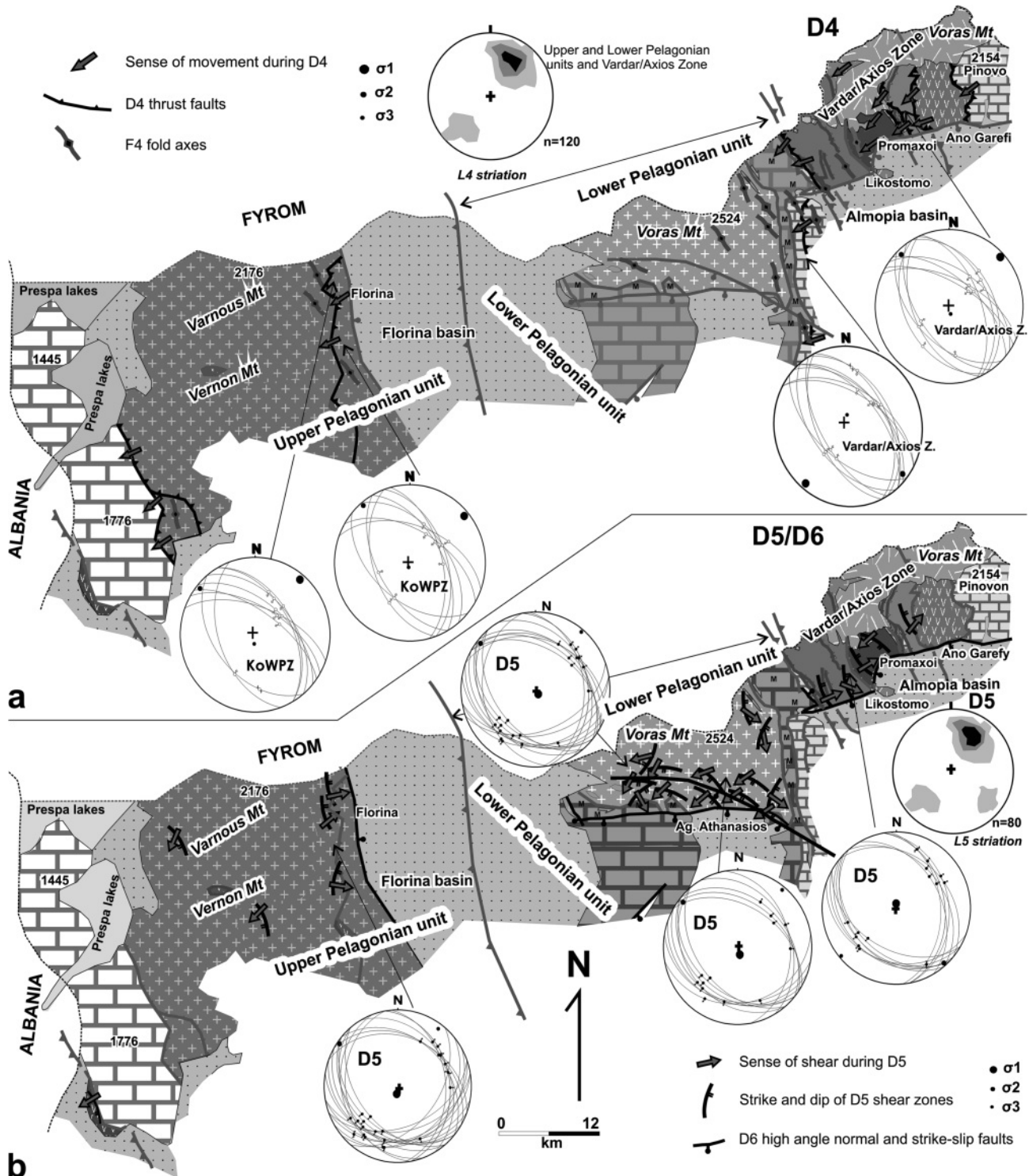


FIGURE 9: Structural elements and kinematics for the D_4 (a) and D_5 (b) events and major high angle normal/oblique faults of the D_6 event (b). L_4 and L_5 striations are shown in Schmidt diagrams (lower hemisphere); contours: 2,5%-5%-7% per 1% area, n=number of measurements. Paleostress data from fault plane analysis are also shown. For explanation, see Fig. 6.

replaced by ilmenite. From the rutile inclusions in D₁ garnet it can be concluded that the high-pressure event started earlier than, or was outlasted by, the D₁ event. The amphibolites contain green amphibole, garnet, white mica, epidote, plagioclase, and biotite.

In the upper tectonostratigraphic levels of the EPZ the calculated temperatures range from 450° to 580° C for a pressure of 10 kb. In the lower levels the temperatures vary between 520° and 620° C for the same pressure. The pressures calculated with the Tweek method range between 8 and 12.5 kb. The Si content of the syn-D₁ white mica varies between 3.2 and 3.4 apfu in average. This indicates minimum pressures from about 6 to 12 kb for the estimated temperatures (Fig. 13a). The decreasing Si content of 0,1 to 0,2 apfu from core to rim in syn-D₁ white mica is ascribed to decreasing pressure during mineral growth (Table II).

The changing composition from core to rim of garnet porphyroblasts reflects a change in temperatures during their evolution (Spear et al., 1990). Increasing X_{Alm} and Mg/(Mg+Fe) ratio as well as decreasing X_{sp} suggest prograde temperature conditions (Table II). Horizontal profiles in some cases indicate either thermal equilibration or growth of these garnets under constant temperature (Fig. 13b,c).

Amphibole compositions plot close to the oligoclase isograd in the diagram of Laird et al. (1984) (Fig. 13d). Ti (0.03-0.06 apfu) and Al^{IV} (0.4-0.6) contents in biotite of the lower structural levels point to low to medium amphibolite facies conditions (T=520° to 600°C) (Table II, Schreurs, 1985).

3.2.3 D₂ EVENT

The syn-D₁ greenschist to amphibolite facies mineral assemblages suffered retrograde, lower greenschist facies overprint during the D₂ event, especially well developed in the higher levels of the EPZ. Sericite, actinolite, chlorite, ilmenite, sphene, epidote, and quartz form the critical syn-D₂ mineral paragenesis. Replacement of D₁ minerals is observed: of biotite and garnet by chlorite and of white mica by sericite in the metapelitic rocks, as well as of hornblende by actinolite and chlorite in the amphibolites (Fig. 7f,g,h).

Using the chlorite thermometer on syn-D₂ chlorites we estimated a temperature range between 280° to 380° C assuming pressure conditions of ca. 4-5 kb (Fig. 13a).

3.2.4 YOUNGER EVENTS

The low-grade metamorphic mylonites to ultramylonites belonging to the D₃ event are characterized by the dynamic recrystallization of quartz (Fig. 7j), quartz ribbons, and a strong lattice preferred orientation of quartz. Feldspar clasts may be broken and show subgrain formation. They are embedded in a dynamically recrystallized quartz and sericite matrix. A well

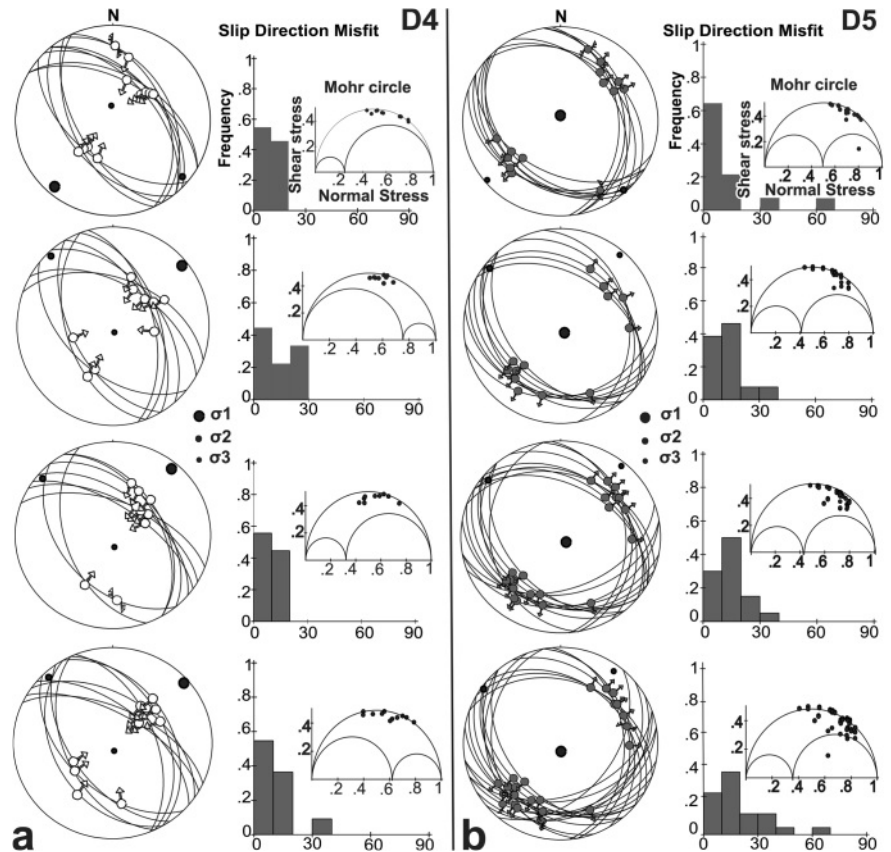


FIGURE 10: Orientation of faults and striae and deduced paleostress field orientation during D₄ (a, left) and D₅ (b, right). Fluctuation histograms of deviation angles (angle between the calculated slip vectors and the measured slickenlines) and Mohr circles are shown.

developed S-C fabric is shown by the orientation of quartz and mica (Fig. 7i,j).

Dynamic recrystallisation of quartz and white mica or chlorite is locally observed along the D₄ thrust faults and D₅ extensional low angle shear zones and related shear bands.

3.3 TIMING OF DEFORMATION

The timing of the tectonometamorphic events is constrained by stratigraphic and geochronological data on syn-tectonic white mica and biotite in relation to the recognised structural events (Yarwood and Dixon, 1977; Koroneos et al., 1993; Galeos et al., 1994; Most, 2003; Brown and Robertson, 2004; Sharp and Robertson, 2006) as well as fission-track dating (Most, 2003; Most et al., 2001; Tables VI, VII; Fig. 13a).

For the HP (blueschist facies) event white mica yielded K/Ar and Ar/Ar ages of ca. 150 Ma (Late Jurassic) (Most, 2003).

The D₁ event has not affected the late Late Jurassic and

Tectonic unit	Lithology	Method	Mineral	Age (Ma)	References
KoWPZ (Upper Pelagonian unit)	Mylonites (FYROM)	K/Ar	wm	35,6±1,4	M
	Gneiss (GR)	K/Ar	wm	75,6±3,0	M
	Gneiss (GR)	K/Ar	wm	40±2,0	M
	Granite gneiss (GR)	Rb/Sr	bi	89,2±26	K
	Granite gneiss (GR)	Rb/Sr	bi	54,5±1,6	K
Blueschists	Blueschist (FYROM)	K/Ar	wm	150±5,1	M
	Blueschist (FYROM)	Ar/Ar	wm	149±1,0	M
EPZ (Lower Pelagonian unit)	Granite gneiss (GR)	Pb/Pb	zirkon	290±5,0	A
	Blueschist (FYROM)	Ar/Ar	wm	148,7±3,3	M
	Micaschist (GR)	K/Ar	wm	145±5,5	M
	Micaschist (GR)	K/Ar	wm	98,6±3,7	M
	Micaschist (FYROM)	Ar/Ar	wm	132,5±2,6	M
			bi	134,0±7,0	
	Micaschist (GR)	K/Ar	wm	128,8±5,4	M
	Micaschist (GR)	K/Ar	wm	131,6±5,0	M
	Micaschist (FYROM)	K/Ar	wm	111,3±3,2	M
	Micaschist (FYROM)	K/Ar	wm	93,8±7,0	M
	Gneiss (FYROM)	K/Ar	wm	147,8±5,7	M
	Gneiss (FYROM)	K/Ar	wm	140,6±5,3	M
	Micaschist (GR)	K/Ar	wm	118,0±4,5	M
	Micaschist (FYROM)	Ar/Ar	bi	103,0±1,5	M
	Micaschist (FYROM)	K/Ar	wm	135,7±5,2	M
	Granite gneiss (FYROM)	k/Ar	wm	134,7±5,1	M
	Granit (FYROM)	K/Ar	bi	128,2±9,0	M
Micaschist (FYROM)	K/Ar	wm	125,9±4,8	M	
		bi	121,4±4,6		
		wm	137,1±5,3	M	
		bi	137,1±5,2		
Vardar/Axios Zone	Micaschist (GR)	Ar/Ar	wm	112,0±1,0	M
	Micaschist (GR)	K/Ar	wm	102,3±3,9	M
	Metaflysch (FYROM)	K/Ar	wm	66,1±2,5	M
	Micaschist (GR)	K/Ar	wm	66,2±2,6	M
	Metaflysch (GR)	K/Ar	wm	64,6±2,5	M
	Flysch pebbles(GR)	K/Ar	wm	132,8±5,0	M
	Flysch pebbles(GR)	K/Ar	wm	144,4±5,0	M

TABLE 6: Geochronological data from the Pelagonian Zone and Vardar/Axios Zone. wm white mica, bi biotite. M: Most (2003), K: Koroneos et al. (1993), A: Avgerinas et al. (2001).

Cretaceous sedimentary sequences sealing the ophiolitic Jurassic nappe stack but is clearly younger than the Variscan orogeny, because it affected post-Variscan (Permian) granites. K/Ar, Ar/Ar, and Rb/Sr isotopic dating on white mica and biotite from the metamorphic rocks of the EPZ yielded a group of ages between 150 to 130 Ma (Most 2003). Due to the attained temperatures during metamorphism, Most et al. (2001) and Most (2003) interpreted these ages as being close to crystallization, although K/Ar and Ar/Ar ages are commonly considered as cooling ages (Jaeger, 1973; Dodson, 1973). Early Cretaceous ages are reported from Pelagonian basement units in Central Greece (Barton, 1976; Yarwood and Dixon, 1977). D₁ ages have been not detected in the KoWPZ and Vardar/Axios Zone.

Tectonic unit	Zircon FT ages (Ma)	Apatite FT ages (Ma)
KoWPZ (Upper Pelagonian unit)	60,5±4,2 (FYROM) 53,3±3,1 (FYROM) 39±2 (GR) 49,0±2,4 (GR) 51,4±4,1 (FYROM)	31±2(GR) 29±5(FYROM)
EPZ (Lower Pelagonian unit)	86,0±4,0 (FYROM) 80±6(FYROM) 63,0±4(FYROM) 71,0±4(FYROM) 66,2 ±3,1 (GR)	46,0±3(FYROM) 32,0±4(FYROM) 41,8± 2,3 (GR)
Vardar/Axios Zone	58±5 (GR)	60±3(GR) 52±3(FYROM)

TABLE 7: Representative zircon and apatite fission track ages from the Pelagonian nappes and the Vardar/Axios basement rocks (Most 2003).

The fossil-dated Late Jurassic-Early Cretaceous transgressive shallow-water carbonate and clastic sequence (Galeos et al., 1994; Brown and Robertson, 2004) seals the ophiolitic nappes (Fig. 3, 6a, 8a) and therefore postdates their emplacement during Middle to Late Jurassic time. This carbonate clastic sequence is in turn overthrust by gneisses and schists of the Vardar/Axios Zone (Peternik unit), thus revealing a syn- to post-Albian tectonic event (Fig. 3, 6a, 8a).

This event appears to correlate with K/Ar and Ar/Ar ages from white mica (Pelagonian nappes and Vardar/Axios Zone) between 110 to 95 Ma (mainly Albian; Koroneos et al., 1993; Most 2003). We interpret these ages as syn-D₂ crystallization ages. A problem about the age determination is arisen due to divergence of the L₁ and L₂ directions in some places. We have not observed on the same sample two different stretching lineations. Furthermore, nor differences of the deviating L₁ and L₂ lineations

in their radiometric ages were found. They have always a Late Jurassic/Early Cretaceous (L₁) or Albian (L₂) age according to the isotopic ages of syn-D₁ and syn-D₂ minerals and their divergence is frequently related to the existence of younger fault zones. May be more detailed radiometric data and structural mapping of the younger fault zones could give better information about this anomalous directions during D₁ and D₂ events.

K/Ar ages of white mica from the KoWPZ and Vardar/Axios Zone between 90 and 70 Ma (Koroneos et al., 1993; Most 2003) are interpreted to report the D₃ event, so that a Late Cretaceous age for the D₃ mylonitic fabric is proposed.

The D₄ semi-ductile to brittle thrusting event took place in Paleocene to Eocene time at already shallow crustal levels. Basement rocks of the Vardar/Axios Zone are thrust over the Maastrichtian to Paleocene flysch (Fig. 8d, 9a). Thrusting of the metamorphic rocks of the Vardar/Axios Zone over the flysch caused local low-grade dynamic recrystallisation of quartz and mica. This event was dated at 65 to 50 Ma by the K/Ar method on fine-grained sericite of the flysch (Most, 2003). These ages are in concordance with stratigraphic as well as zircon and apatite fission-tracks ages (Table VII; Most, 2003).

Zircon fission-track ages between 85 and 65 Ma from EPZ samples (Most, 2003) show that this deeper structural level of the Pelagonian edifice had already cooled below ca. 240° C in late Late Cretaceous time. The oldest zircon FT ages (85 Ma) are derived from the innermost parts of the EPZ while younger FT ages dominate towards its eastern (72 Ma) and

western (63 Ma) margins (Most, 2003). Moreover gneiss and schist pebbles derived from the EPZ and contained in Maastriichtian to Paleocene flysch, show the imprint of the D₁ event. Therefore, parts of the EPZ basement had already been exhumed at that time. Zircon fission-track ages from the KoWPZ

are between 53 and 40 Ma and from the Vardar/Axios Zone between 80 and 60 Ma (Most, 2003).

Apatite fission-track ages in the KoWPZ, EPZ and Vardar/Axios Zone cluster between 60 and 30 Ma (Most, 2003). They continuously decrease from the Vardar/Axios Zone (ca. 60 Ma)

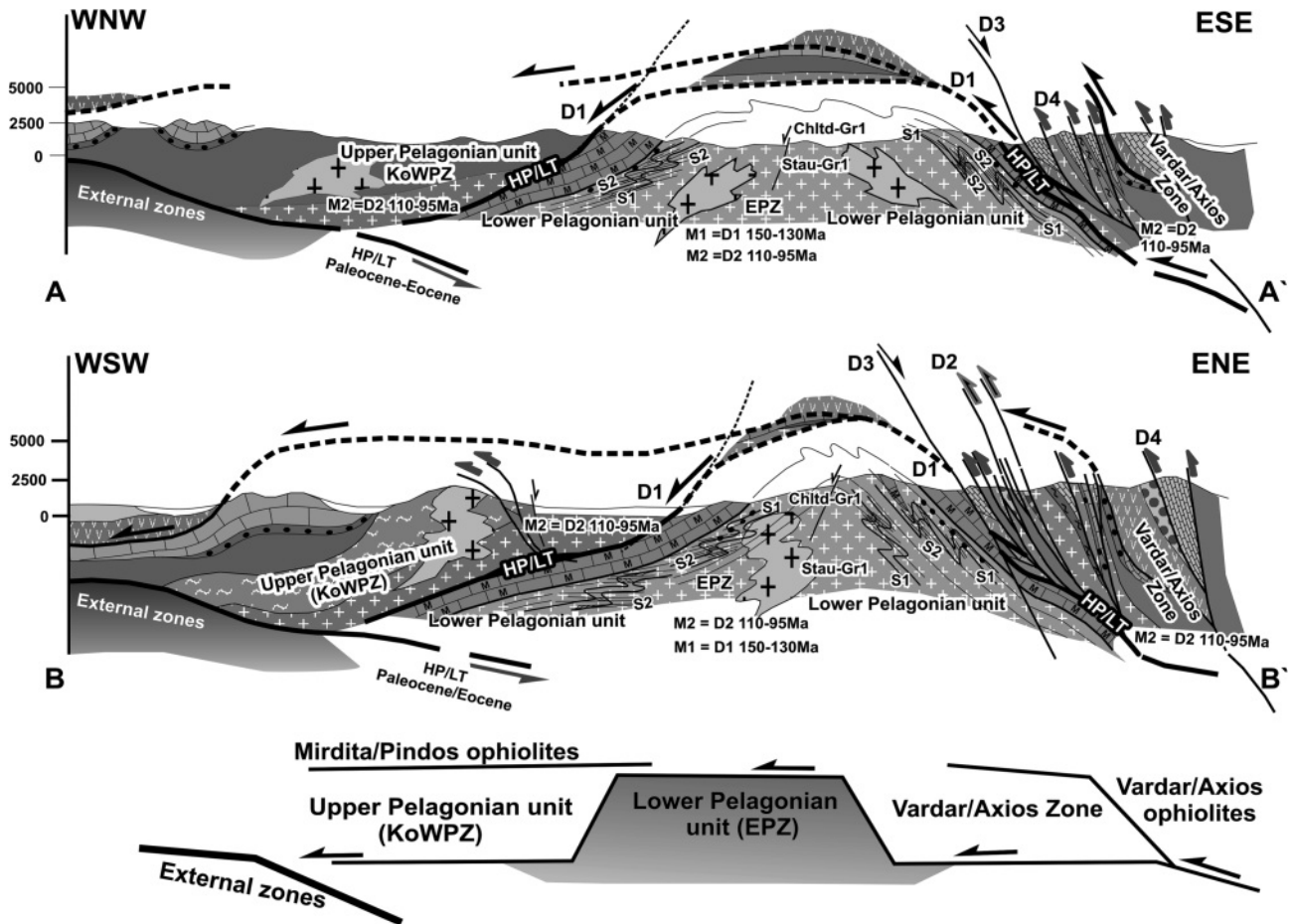


FIGURE 11: Geological cross sections through the northern Pelagonian nappes and the Vardar/Axios Zone showing structural relationships and stages of deformation in northern part of study area (FYROM) (A -A') and southern part of study area (northern Greece) (B -B'). For location of section, see Fig. 2. Legend as in Fig. 3.

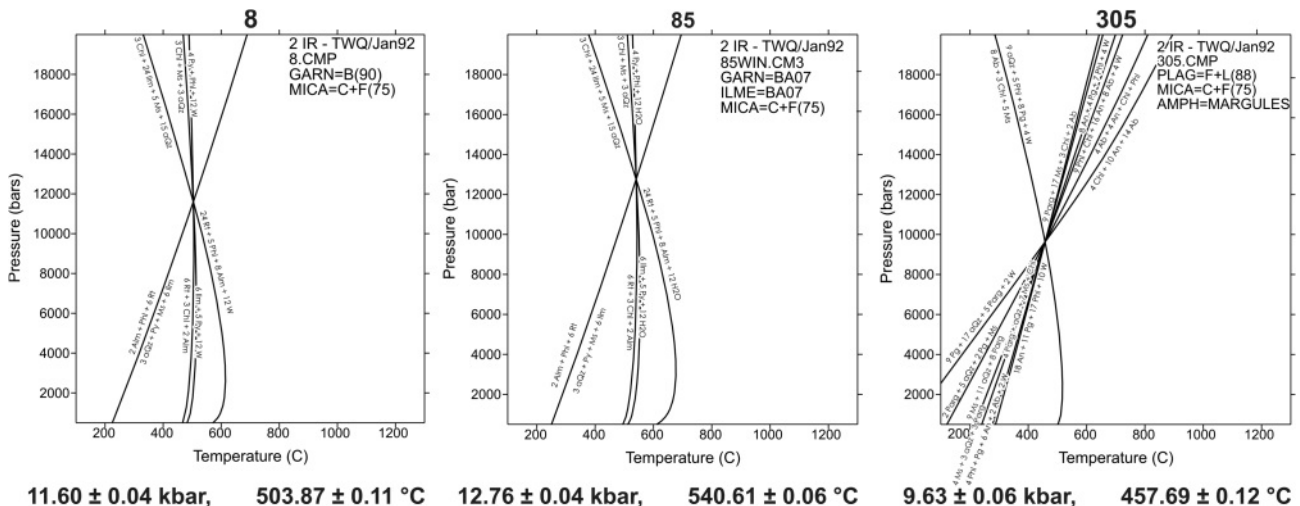
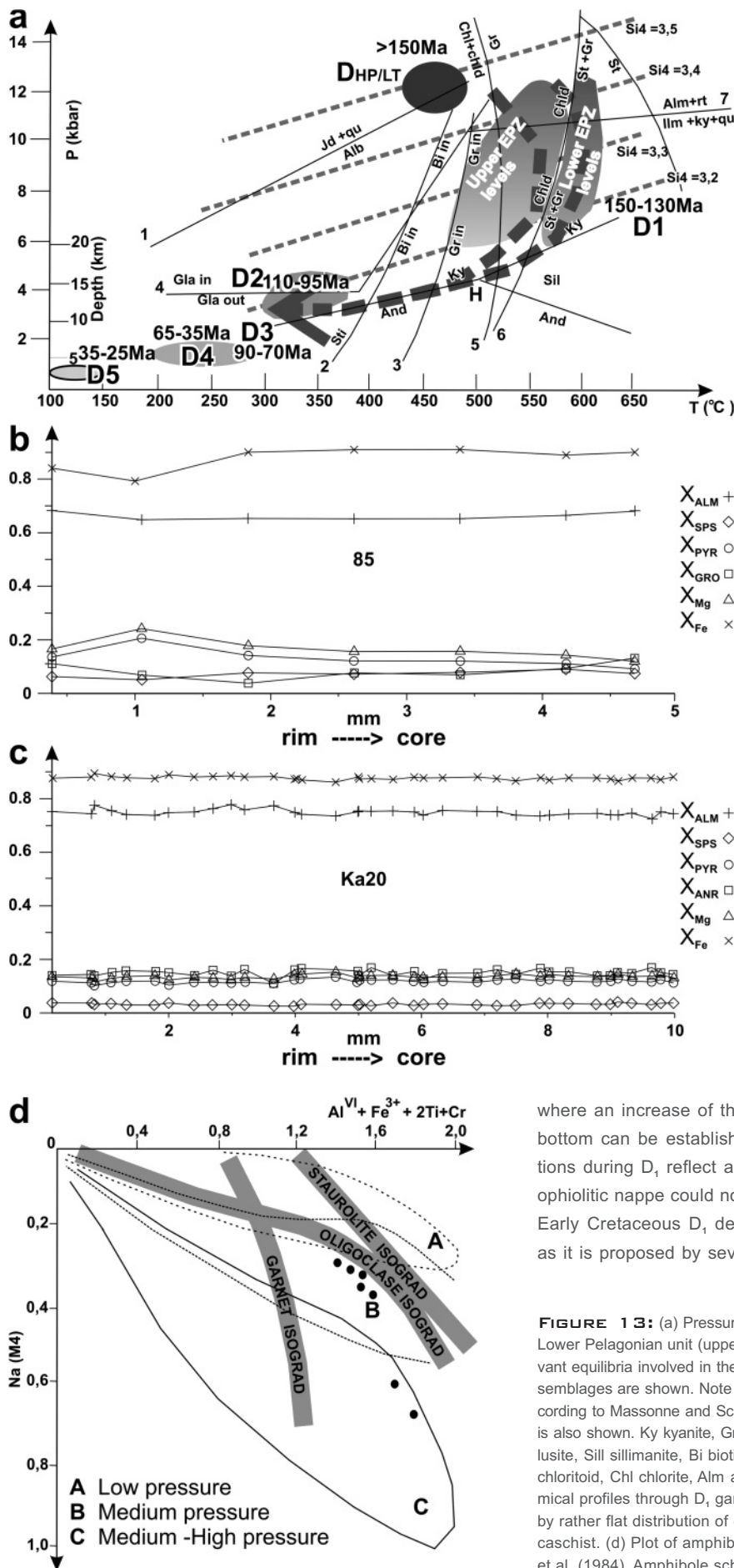


FIGURE 12: Representative examples of thermobarometric results deduced from the Tweek programm (Bermann, 1991). Samples 8, 85: garnet-chloritoid micaschists; 305: amphibole schist. Lower Pelagonian unit.



through the EPZ (46-33 Ma) to the KoWPZ (ca. 30 Ma). This indicates progressive exhumation and cooling below ca. 110° C from east to west. Westward migration of deformation during Tertiary time was already proposed by Jacobshagen et al. (1978), Schermer et al. (1990), Kiliass et al. (1991, 1999) and Schermer (1993).

Ar/Ar radiometric dating of white mica in the Olympos and Pieria mountains in the central Pelagonian zone to the south of the study area (Fig. 2) show a broadly continuous period of deformation between ca. 65 and 40 Ma, associated with high-pressure metamorphism, ductile deformation and mylonite formation. This area belongs to the internal blueschist belt of the Hellenides (Fig. 1) and forms the lowermost structural levels of the Pelagonian nappe (Schermer et al., 1990; Kiliass et al., 1991; Schermer, 1993; Lips et al., 1998).

For the D₅ event (normal shear zones and faults) an age between Oligocene and beginning Miocene is suggested because it is younger than the D₄ event and older than the D₆ event. The D₆ event, which is related to Neogene-Quaternary basin formation, started in Miocene time and finds its expression in still active faults.

3.4 TECTONIC SETTING

D₁ is recognized only in the EPZ where an increase of the metamorphic grade from tectonic top to bottom can be established. Furthermore, the metamorphic conditions during D₁ reflect a thick crustal stack above the EPZ. A thin ophiolitic nappe could not result along the described Late Jurassic/Early Cretaceous D₁ deformation and associated metamorphism, as it is proposed by several studies (Barton, 1976; Yarwood & Di-

FIGURE 13: (a) Pressure-temperature-time-deformation relationship of the Lower Pelagonian unit (upper and lower structural levels separated). The relevant equilibria involved in the stability field of the syn-deformational mineral assemblages are shown. Note stability curves for Si=3,2 to 3,5 of white mica according to Massonne and Schreyer (1987). P-T field for the high-pressure event is also shown. Ky kyanite, Gr garnet, St staurolite, Gla glaucophane, And andalusite, Sill sillimanite, Bi biotite, Sti stilpnomelane, Jd jadeite, Qu quartz, Chld chloritoid, Chl chlorite, Alm almandine, Rt rutile, Ilm ilmenite. (b) and (c) Chemical profiles through D₁ garnets of the Lower Pelagonian unit, characterized by rather flat distribution of element contents: 85, Ka20: garnet-chloritoid mica-schist. (d) Plot of amphibole microprobe analyses in the diagram of Laird et al. (1984). Amphibole schist. Lower Pelagonian unit.

xon, 1977). The blueschist belt around the boundaries of the EPZ is of about the same age as, or slightly older than, the syn- D_1 metamorphism. D_{HP} and D_1 are related to subduction, nappe stacking and crustal thickening (Fig. 6a, 8a, 11).

Further nappe stacking took place during the D_2 event as it is clearly evidenced by thrusting of the Vardar/Axios basement over the Late Jurassic to Aptian/Albian clastic sediments and shallow-water limestones which are in turn transgressively overlying the obducted ophiolites (Fig. 6a, 8b, 11). The associated metamorphism did not exceed lower to middle greenschist facies conditions. It is recognized in the upper structural parts of the East Pelagonian Zone and clearly penetrative in the whole Vardar basement rocks and the KoWPZ.

Thrusting during D_1 and D_2 was generally NW-directed. Some SE-ward sense of movement represents local backthrusts and strain partitioning. Deviations from the main direction of transport as reported for both events in some places are probably due to local complications and later block rotations as a result of younger faults activation. We do not consider them to be of regional importance.

The D_3 mylonitic shear zones generally show a top-to-NE normal sense of movement and are not associated with folds as typically observed in the D_1 and D_2 contractional structures. D_3 forms discrete low-angle shear zones dominating in the Vardar/Axios basement rocks and the KoWPZ. According to their geometry and kinematics we interpret the D_3 mylonitic shear zones as extensional structures related to ca. NE-SW oriented crustal stretching and unroofing (Fig. 6b, 8c, 11). They are of Late Cretaceous age and probably associated with basin formation and the sedimentation of Late Cretaceous limestones and Maastrichtian to Paleocene flysch.

Ratschbacher et al. (1989) and Neubauer et al. (1995) showed that Late Cretaceous extension associated with exhumation of metamorphic rocks and formation of the Gosau basin are also a prominent feature in the highest tectonic unit (the Austroalpine mega-unit) in the Eastern Alps.

D_4 deformation is clearly related to a contractional regime and intense SW-ward imbrication of all tectonic units. Metamorphic basement rocks of the Vardar/Axios Zone were thrust over the Maastrichtian to Paleocene flysch. Thrust sheets of Mesozoic/Tertiary sequences and ophiolites were formed within the Vardar/Axios Zone (Fig. 8d, 9a, 11).

D_5 fault zones always display a normal component of displacement indicating an extensional tectonic setting under brittle conditions. Extension was mainly NE-SW oriented (Fig. 9b, 10b). The final stage of deformation (D_6) is related to a transtensional or extensional regime (Pavlidis et al. 1990) and responsible for intense dissection of the whole nappe pile.

4. DISCUSSION OF THE GEODYNAMIC EVOLUTION AND CONCLUSIONS

Our detailed structural and petrological data combined with geochronological investigation concerning the northern Pelagonian nappe pile and the neighbouring Vardar/Axios Zone in northern Greece and FYROM allows to constrain the geome-

try and kinematics of deformation, as well as the structural evolution during the Alpine orogeny.

According to our study, the Pelagonian nappe system in northern Greece and FYROM can be divided at minimum into two distinct tectonostratigraphic units, the Lower (EPZ) and the Upper (KoWPZ) Pelagonian unit. The KoWPZ seems to be rooted between EPZ and Vardar/Axios Zone, where only intensely imbricated remnants of slices are recognized. The Paleozoic sequence and the gneisses and schists of the Vardar/Axios Zone are considered to represent the equivalents of the KoWPZ, the connection being eroded in the Pelagonian dome structure (Fig. 2, 11).

This scenario proves the duplication of the Pelagonian sequence due to Middle Jurassic to Early Cretaceous nappe stacking towards WNW to NW (D_{HP} and D_1 event). Nappe stacking was related to plate convergence, inneroceanic thrusting in the western Vardar/Axios Ocean and ophiolite obduction on the top of the Pelagonian Continent. (Fig. 11, 14a,b; Roddick et al., 1979; Spray and Roddick, 1980; Vergely, 1984; Dimo, 1997; Pamic, 2002; Brown and Robertson, 2004; Sharp and Robertson, 2006; Karamata, 2006; Gawlick et al., 2008).

An important point for the reconstruction of the structural evolution of the study area are the late Late Jurassic to Early Cretaceous clastic sediments and shallow-water limestones transgressively overlying the ophiolites providing an upper limit for ophiolite emplacement. They indicate that the ophiolites were emplaced before the Kimmeridgian (compare Schlagintweit et al., 2008) (Fig. 14b,c). D_1 thrusting and metamorphism in deeper structural levels occurred almost simultaneously with the early sedimentation of this clastic sedimentary sequence, possibly with coeval crustal extension at the top of the nappe pile (Fig. 14c).

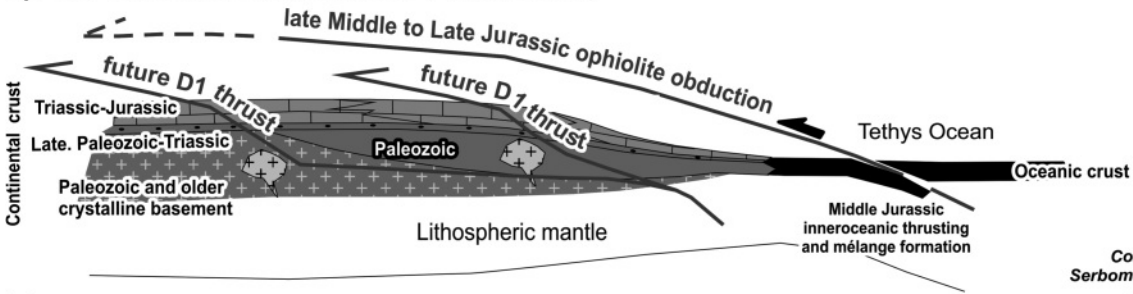
An equivalent sequence of shallow-water limestones and clastic sediments, the Kurbnesh series, is recognized further to the west in Albania, where it seals the Mirdita ophiolitic nappe stack (Gawlick et al., 2008). The Mirdita ophiolites overlie the Triassic-Jurassic shallow- and deep-water carbonates of the KoWPZ (Robertson and Shallo, 2000; Kiliyas et al., 2001; Shallo and Dilek, 2003) (Fig. 2, 3, 11).

Plate convergence and thrusting continued during Aptian to Albian time (ca. 110 to 95 Ma) with the same kinematics as during the D_1 event (D_2 event: Fig. 11, 14d).

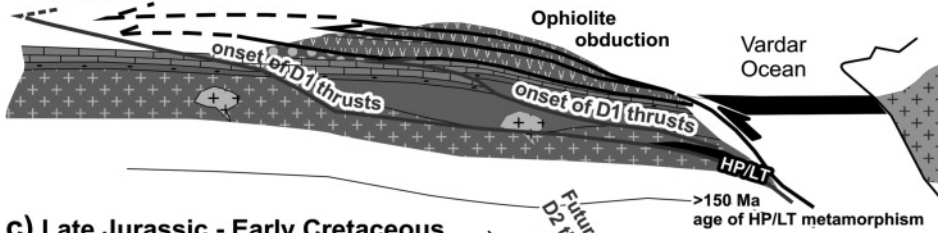
D_1 and D_2 nappe stacking was followed by D_3 low angle normal discrete mylonitic shear zones in Late Cretaceous time. They were associated with basin formation and sedimentation of Late Cretaceous neritic limestones and Maastrichtian to Paleocene flysch (Fig. 14e). Parts of the EPZ were firstly exhumed at this time possibly related to the D_3 extensional regime.

Simultaneously with Late Cretaceous to Paleocene extension and sedimentation on top of the tectonically upper units, thrusting in the tectonically lower and more external (more western) units took place. This thrusting process was associated with the internal high-pressure metamorphic belt (Fig. 2, 14e; Schermer et al., 1990; Kiliyas et al., 1991; Lips et al., 1998). Schermer (1990) relates the formation of the internal

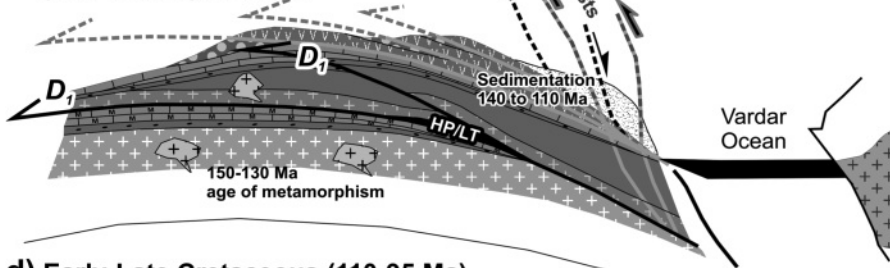
a) Late Triassic to Early Jurassic (~220-175 ma)



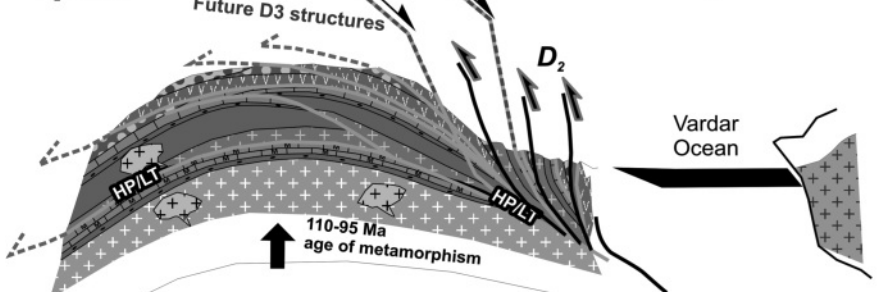
b) Middle-Late Jurassic (160-150 Ma) HP event



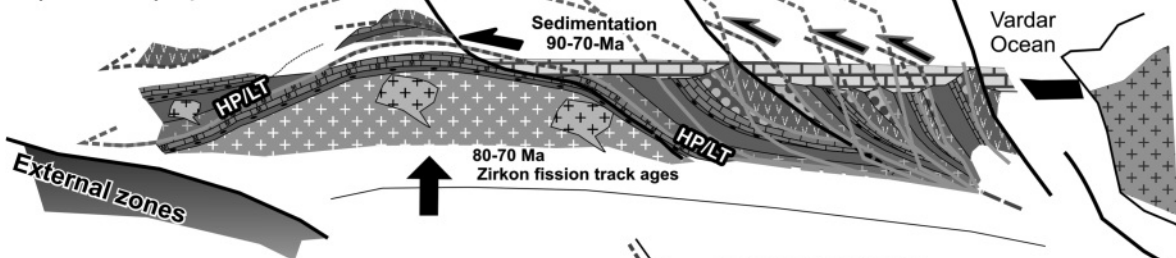
c) Late Jurassic - Early Cretaceous (150-130 Ma) D1 event



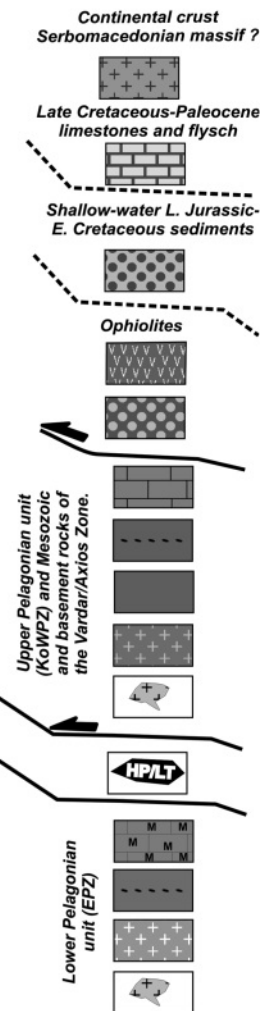
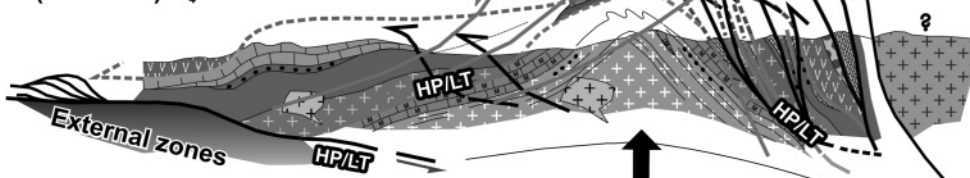
d) Early-Late Cretaceous (110-95 Ma) D2 event



e) Late Cretaceous (90-70 Ma) D3 event



f) Paleocene-Eocene (65-35 Ma) D4 event



HP belt to intra-continental subduction.

D_4 thrusting and nappe stacking was characterized by very-low grade metamorphism of the imbricated slices (Fig. 11, 14f). The doming of the present antiformal structure of the EPZ was probably the result of D_4 shortening. The described distribution of the zircon FT ages in the EPZ shows that the EPZ did not evolve as a metamorphic core complex (Most, 2003). In the case of a metamorphic core complex extension plays an important role (Platt, 1993) and the youngest cooling ages are located in the centre of the dome (e. g., Tauern metamorphic core complex, Eastern Alps: Ratschbacher et al., 1989; Rhodope metamorphic core complex, Northern Greece: Dinter and Royden, 1993; Kiliias et al., 1999). D_4 is related to continuous subduction of continental crust beneath the tectonic lower part of the Pelagonian nappe and the creation of the internal HP belt in the Olympos-Ossa area (Godfriaux, 1968; Katsikatsos et al., 1982; Schermer et al., 1990; Kiliias et al., 1991; Lips et al., 1998), on Evvia island (Katsikatsos, 1977; Xypolias et al., 2003), and in the Cyclades (Duerr et al., 1978; Andressen et al., 1979; Schliestedt et al., 1987) (Fig. 1). D_4 is also responsible for the final W- to WSW-ward emplacement of the Internal Hellenides (Pelagonian nappes) upon the External Hellenides in Eocene-Oligocene time. This means that, from the Late Cretaceous to the Eocene, there was a continuous period of deformation prograding from the tectonic top to the tectonic bottom and associated with nappe stacking and HP metamorphism (Fig. 14e,f).

Detailed discussion and analysis of paleogeographic settings for the evolution of one or more ocean basins in the Hellenides (Vergely, 1984; Mountrakis, 1986; Jones and Robertson, 1991; Robertson and Shallo, 2000; Shallo and Dilek, 2003; Rassios and Moores, 2006; Gawlick et al., 2008; Rassios and Dilek, 2009; Papanikolaou, 2009) is outside of the aim of our study. Nevertheless, we like to point out that the suture zone between External and Internal Hellenides is free of ophiolites and all the Pelagonian nappe pile between External Hellenides and the basal ophiolite nappe is continental in origin. Furthermore, the main NW-directed thrusting polarity during the D_1 and D_2 events, as documented here, indicates that the ophiolitic nappes on top of the Pelagonian nappes should be rooted in the Tethys (Vardar/Axios) ocean basin to the east of the Pelagonian continent. Ophiolite emplacement was consistently

more or less towards the west (Fig. 11, 14). All this suggests that the Pelagonian continental block was not separated from the External Hellenides by an oceanic lithosphere during Alpine orogeny. Therefore, we do not see an independent Pindos Ocean neither in Triassic nor in Jurassic period.

Moreover, we did not observe important eastward thrusting during the different stages of Alpine deformation from Jurassic to Tertiary time, as referred to by several authors for other regions in the Hellenides (Barton, 1976; Doutsos et al., 1993; Lips et al., 1998; Sharp and Robertson, 2006). Eastward sense of shear of high-T mylonitic shear zones of the ophiolites on top of the western margin of the Pelagonian realm was also described by Rassios and Moores (2006) and Rassios and Dilek (2009) implying E-(NE-)ward tectonic emplacement of the ophiolites but without presenting any combined structural analysis of the Pelagonian units below the ophiolitic nappe. In our study region NE-ward sense of movement was related to extensional mylonitic shear zones (D_3 event) and backthrusting during D_4 nappe stacking. Moreover, overall E-(NE-) ward subduction of the Tethyan paleogeographic elements in the Hellenides since the Jurassic, which resulted in the closure of the Tethys oceanic basin (Ricou et al., 1998; Schmid et al., 2008; Papanikolaou, 2009) can hardly explain an E-(NE-) directed tectonic emplacement of the ophiolites over the adjacent continental margin.

The same scenario with general W-directed emplacement of the large ophiolite bodies that derived from one single ocean in the east is documented in Albania. There the large Mirdita ophiolite nappes to the west of the KoWPZ are far-travelled parts of the Vardar/Axios (Neotethys) ocean, brought into its present position by W-ward thrusting in Middle to Late Jurassic time (Hoxha, 2001; Kiliias et al., 2001; Gawlick et al., 2008).

Deformation continued during Oligocene to Early Miocene time (D_5 ; Fig. 14f). In higher structural levels of the Pelagonian nappes and the Vardar/Axios Zone brittle conditions prevailed and created cataclases and ultracataclases in low-angle extensional shear zones. Simultaneous ductile deformation with mylonites and a constant top-to-the-SW normal sense of shear associated with subhorizontal extension is reported in tectonic deeper levels of the Pelagonian nappe near its contact to the underlying External Hellenides (Sfeikos et al., 1991; Kiliias et al., 1991; Sfeikos, 1992; Schermer, 1993). This process is related to Oligocene/Miocene collapse of the Pelagonian nappe pile, tectonic thinning, and unroofing and exhumation of tectonically deeper levels of the External Hellenides (e. g., Olympos-Ossa window). W- to SW-directed thrusting towards the foreland and the most external parts of the Hellenides continued during this period (Schermer et al., 1990; Sfeikos et al., 1991; Kiliias et al., 1991, 2002; Schermer, 1993).

From Miocene to present time high-angle normal to oblique-normal faults (D_6) affected all units. This extensional event was responsible for the formation of the Neogene basins and steered the unroofing history of the region.

FIGURE 14: a. Schematic crustal-scale transect indicating paleogeographic relations along Pelagonian continental margin during Triassic to Early/Middle Jurassic time. Deformation started about late Early-Middle Jurassic related to plate convergence and inneroceanic thrusting in the Vardar/Axios Ocean. b to f. Schematic crustal-scale transects showing progression of deformation and kinematic history of the Pelagonian and Vardar/Axios Zones from Middle-Late Jurassic to Oligocene-Miocene time (D_{HP} , D_1 , D_2 , D_3 , D_4 and D_5). Contraction and nappe stacking was associated with Late Jurassic to Early Cretaceous clastic and shallow-water carbonate sedimentation (b and c). D_2 contraction followed (d). Late Cretaceous Extension (D_3) associated with basin formation and crustal unroofing (e) was replaced by D_4 contraction and imbrication of all tectonic units during Paleocene to Eocene time (f). Future D_5 extensional structures are also shown (f). Legend as in Fig.3.

ACKNOWLEDGMENTS

The work is part of a cooperative study between the institute of Geology, University of Tuebingen, Germany and the Institute of Geology and Paleontology, University of Thessaloniki, Greece. We thank Sylvia Mettasch for her assistance to carry out a series of microprobe analyses in the University of Tuebingen. We also thank two anonymous referees for their critical comments, as well as Bernhard Grasemann and Hugh Rice for editorial assistance.

REFERENCES

- Anders, B., Reischmann, T., Kostopoulos, D. und Poller, U., 2006. The oldest rocks of Greece: first evidence for a Precambrian terrane within the Pelagonian zone. *Geological Magazine*, 143, 41-58.
- Anders, B., Reischmann, T., Kostopoulos, D., Lehnert, O., Matukov, D. and Sergeev, S., 2007. Zircon geochronology of basement rocks from the Pelagonian Zone. Greece: Constraints on the pre-Alpine evolution of the westernmost Internal Hellenides. *International Journal of Earth Sciences*, 96, 639-661.
- Andressen, P.A., Boerlijck, N.A.I. M., Hebeda, E.H., Priem, H. N.A., Verdurmen E.A.T. and Verschure, R.H., 1979. Dating the events of metamorphism and granitic magmatism in the Alpine Orogen of Naxos (Cyclades, Greece). *Contributions to Mineralogy and Petrology*, 69, 215-225.
- Angelier, J., Goguel J., 1979. Sur une methode simple de détermination des axes principaux des contraintes pour une population de failles. *Compte Rendue Academie des Sciences*, 282, 307-310.
- Angelier, J. and Mechler, P., 1977. Sur une méthode graphique de recherché des contraintes principales également utilisable en tectonique et en seismologie: la méthode des diedres droits. *Bulletin de la Société Géologique de France*, 19, 1309-1318.
- Arsovski, M. and Dumurdzanov, N., 1984. Recent findings of the structure of the Pelagonian antidiorium and its relation with the Rhodopean and Serbian Macedonian Massif. *Geologica Macedonica*, 2, 15-22.
- Arsovski, M., Dumurdzanov, N., Hristov, S., Ivanova, N., Petkovski, P. and Stojanov, R., 1977. Correlation of the Pre-Cambrian complexes of the Pelagonian Massif, Vardar zone and Serbo-Macedonian massif. In: Kallergis (ed). *Pocceedings of the 6th colloquium on the geology of the Aegean region*, Athens, pp. 549-557.
- Avgerinas, A., Kiliias, A., Koroneos, A., Mountrakis, D., Frisch, W., Dunkl, I. and Most, T., 2001. Cretaceous structural evolution of the Pelagonian crystalline in Western Voras Mt. (Macedonia, Northern Greece). *Bulletin of Geological Society of Greece*, 34, 129-136.
- Barton, C.M., 1976. The tectonic vector and emplacement age of an allochthoyous basement slice in the Olympos area, NE Grec. *Bulletin de la Societe Geologique de France*, 7, 253-258.
- Berman, R.G., 1991. Thermobarometry using multiequilibrium calculations: A new technique with petrological applications. *Canadian Mineralogist*, 29, 833-855.
- Bernouli, D. and Laubscher, H., 1972. The palinspastic problem of the Hellenides. *Eclogae Geologicae Helveticae*, 65, 107-118.
- Blencoe, J.G., Guidotti, C. V. and Sassi F.P., 1994. The paragonite-muscovite solvus: II. Numerical geothermometers for natural, quasibinary paragonitemuscovite pairs. *Geochim Cosmochim Acta*, 58, 2277-2288.
- Borsi, S., Ferrara, G., Mercier, J. and Tongiorgi, E., 1966. Age stratigraphique et radiometrique jurassique superieur d' un granite des zones internes des Hellenides (granite de Fanos, Macedoine, Greece). *Revue de Geographie Physique et Géologie*, 2, 279-287.
- Bortolotti, V., Marroni, M., Pandolfi, L. and Principi, G., 2005. Mesozoic and Tertiary tectonic history of the Mirdita ophiolites, northern Albania. *The Island Arc* 14: 471-493.
- Brown, S.A.M. and Robertson, A.H.F., 2004. Evidence for the Neotethys ocean rooted in the Vardar zone: evidence from the Voras Mountains, NW Greece. *Tectonophysics*, 381, 143-173.
- Brunn, J.H., 1956. Contribution à l' étude géologique du Pinde septentrional et d' une partie de la Macédoine occidnetale. *Annale Géologique de Pays Hellénique*, 7, 1-358.
- Burchfiel, B.C., 1980. Eastern European Alpine system and the Carpathian orocline as an example of collision tectonics. *Tectonophysics*, 63, 31-61.
- Cathelineau, M., 1998. Cation site occupancy in chlorites and illites as a function of temperature. *Cley Minerals* 23, 471-485.
- De Bono, R., Martini, L., Zaninetti, F., Hirsch, G., Stampfli, I. and Vavassis, A., 2001. Permo-Triassic stratigraphy of the Pelagonian Zone in central Evia island (Greece). *Eclogae Geologicae Helveticae*, 94, 213-223.
- Dimo, A., 1997. Le mécanisme de mise en place des ophiolites d' Albanie. PhD Thesis, University of Paris – Sud, Paris, 308 pp and annexes.
- Dinter, A.D., and Royden, L., 1993. Late Cenozoic extension in Northeastern Greece: Strymon Valley detachment and Rhodope metamorphic core complex. *Geology*, 21, 45-48.
- Dodson, M. 1973. Closure temperature in cooling geochronological and petrological systems. *Contributions to Mineralogy and Petrology*, 40, 259-274.

- Dumurdzanov, N., Hritov, S., Pavlovski, B., and Ivanova, V., 1976. Explanatory note of the general geological map of SRFJ, Sheet Vitoliste and Kajmakcalan. Federal Geological Survey of Yugoslavia, Belgrade, scale 1:100.000.
- Dumurdzanov, N., Serafimovski, T. and Burchfiel, B.C., 2005. Cenozoic tectonic of Macedonia and its relation to the South Balkan extensional regime. *Geosphere*, 1, 1-22.
- Duerr, S., Altherr, R., Keller, J., Okrusch, M., and Sidedl, E., 1978. The median Aegean Crystalline Belt: stratigraphy, structure, metamorphism, magmatism. In: H. Cloos, D. Roeder and K. Schmidt (eds), *Alps, Apennines, Hellenides*, Schweizerbart'sche Verlagsbuchhandlung, Stuttgart, pp. 455-477.
- Duyster, J., 2000. Stereo Nett, Microsoft Corp., Universitaet Bochum.
- Fassoulas, Ch., Kiliias, A. and Mountrakis D., 1994. Postnappe stacking extension and exhumation of highpressure/low temperature rocks in the island of Crete, Greece. *Tectonics*, 13, 127-138.
- Ferry, J.M. and Spear, F.S., 1978. Experimental calibration of the partitioning of Fe and Mg between biotite and garnet. *Contributions to Mineralogy and Petrology*, 66, 113-117.
- Gawlick, H.J., Frisch, W., Hoxha, L., Dumitrica, P., Krystyn, L., Lein, R., Missoni, S. and Schlagintweit, F., 2008. Mirdita zone ophiolites and associated sediments in Albania reveal Neothethys Ocean origin. *International Journal of Earth Sciences*, 94, 865-881.
- Geleos, A., Pamoni-Papaioannou, F., Tsaila-Monopolis, S., Turneek, D. and Joakim, Chr., 1994. Upper Jurassic -Lower Cretaceous "molassic type" sedimentation in the western part of Almopia subzone, Loutra Aridea unit (Northern Greece). *Bulletin of Geological Society of Greece*, 31, 171-184.
- Godfriaux, J., 1968. Etude géologique de la région de l' Olympe (Grèce). *Annale Géologique de Pays Hellénique*, 19, 1-271.
- Grambling, A.J., 1990. Internally-consistent geothermometry and H₂O barometry in metamorphic rocks: the example garnet-chlorite-quartz. *Contributions to Mineralogy and Petrology*, 105, 617-628.
- Himmerkus, F., Reischmann, T. and Kostopoulos, D., 2006. Proterozoic and Silurian basement units within the Serbo-Macedonian Massif, northern Greece: the significance of terrane accretion in the Hellenides. *Geological Society of London, Special Publication*, 260, 35-50.
- Hoxha, L., 2001. The Jurassic-Cretaceous orogenic event and its effects in the exploration of sulphide ores, Albanian Ophiolites, Albania. *Eclogae Geologicae Helvetiae*, 94, 339-350.
- Hynes, A. and Forest, R.C., 1988. Empirical garnet-muscovite geothermometry in low-grade pelites, Selwyn Range (Canadian Rockies). *Journal of Metamorphic Geology*, 6, 297-309.
- Indares, A. and Martignole, J., 1985. Biotite –garnet geothermometry in the granulite facies: the influence of Ti and Al in biotite. *American Mineralogist*, 70, 272-278.
- Jacobshagen, V., 1986. *Geologie von Griechenland*. Beitrage zur regionalen Geologie der Erde. Gebrueder Borntraeger Verlag, Berlin, 363 pp.
- Jacobshagen, V., Duerr, F., Kockel, K., Kopp, K.O., Kowalczyk, G., Berckhemer, H. and Buttner, D., 1978. Structure and geodynamic evolution of the Aegean region. In: H. Cloos, D. Roeder and K. Schmidt (eds), *Alps, Apennines, Hellenides*. E. Schweizerbart'sche Verlagsbuchhandlung, Stuttgart, pp. 537-564.
- Jaeger, E., 1973. Die alpine Orogenese im Lichte der radiometrischen Altersbestimmung. *Eclogae Geologicae Helvetiae*, 66, 11-21.
- Jones, G. and Robertson, A.H.F., 1991. Tectonostratigraphy and evolution of the Mesozoic Pindos ophiolite and related units, Northwestern Greece. *Journal of Geological Society of London*, 148, 267-288.
- Karamata, S., 2006. The geological development of the Balkan Peninsula related to the approach, collision and compression of Gondwana and Eurasian units. In: A.H.F. Robertson and D. Mountrakis (eds), *Tectonic Development of the Eastern Mediterranean Region*. Geological Society of London, Special Publication, 260, pp. 373-412.
- Katerinopoulos A., 2008. Variscan basic dykes in the Pelagonian (Northern Greece and south FYROM): Geodynamic significance based on petrological, geochemical and geochronological studies. *Chemie der Erde*, 68, 93-103.
- Katsikatsos, G., 1977. La structure tectoniques d' Attique et de l' ile d' Eubée. In: G. Kallergis, (ed). *Proceedings of the 6th colloquium on the geology of the Aegean region*, Athens, 221-228.
- Katsikatsos, G., Migiros, G. and Vidakis, M., 1982. La structure géologique de la region de la Thèssalie orientale, Greece. *Annale Societe Géologique du Nord*, 101, 177-188.
- Kiliias, A. 1991. Transpressive Tectonik in den zentralen Helleniden. Aenderung der Translationpfade durch die Transgression Nord-Zentral Griechenland). *Neues Jahrbuch fuer Geologie und Palaeontologie Monatshefte*, 5, 291-306.
- Kiliias, A. and Mountrakis, D., 1987. Zum tektonischen Bau der Zentral-Pelagonischen Zone (Kamvounia Gebirge, N. Griechenland). *Zeitschrift der Deutschen Geologischen Gesellschaft*, 138, 211-237.
- Kiliias, A., Fassoulas, Ch., Priniotakis, M., Frisch, W. and Sfeikos, A., 1991. Deformation and HP/LT metamorphic conditions at the tectonic window of Kranea W. Thessaly, N. Greece). *Zeitschrift der Deutschen Geologischen Gesellschaft*, 142, 87-96.

- Kilias, A., Tranos, M., Mountrakis, D., Shallo, M., Marto, A. and Turku, I., 2001. Geometry and kinematics of deformation in the Albanian orogenic belt during the Tertiary. *Journal of Geodynamics*, 31, 169-187.
- Kilias, A., Falalakis, G. and Mountrakis, D., 1999. Cretaceous Tertiary structures and Kinematics of the Serbomacedonian metamorphic rocks and their relation to the exhumation of the Hellenic Hinterland Macedonia, Greece). *International Journal of Earth Sciences*, 88, 513-531.
- Kilias, A., Tranos, M.D., Orozco, M., AlonsoChaves, F.M. and Soto, J.I., 2002. Extensional collapse of the Hellenides: A review. *Revista de la Sociedad Geologica de Espana*, 15, 129-139.
- Koroneos, A., Christofides, G., Del Moro, A., and Kilias, A., 1993. Rb-Sr geochronology and geochemical aspects of the Eastern Varnountas plutonite (NW Macedonia, Greece). *Neues Jahrbuch fuer Mineralogische Abhandlungen*, 165, 297-315.
- Kotopouli, C.N., Pe-Piper, G. and Pe-Piper, D.J.W., 2000. Petrology and evolution of the Herzynian Pieria Granitoid Complex (Thessaly, Greece): Paleogeographic and geodynamic implications. *Lithos*, 80, 137-152.
- Laird, J., Lamphere, M.A., and Albee, A.L., 1984. Distribution of Ordovician and Devonian metamorphism in mafic and pelitic schists from northern Vermont. *American Journal of Sciences*, 284, 376-413.
- Lips, A.L.W., White, S.H. and Wijbrans, J.R., 1998. $^{40}\text{Ar}/^{39}\text{Ar}$ laserprobe direct dating of discrete deformational events; a continuous record of early Alpine tectonics in the Pelagonian zone, NW Aegean area Greece. *Tectonophysics*, 298, 133-103.
- Lister, G. and Snoke A., 1984. SC Mylonites. *Journal of Structural Geology*, 12, 379-411.
- Lister, G.S., Banga, G. and Feenstra, A., 1984. Metamorphic core complex of Cordilleran type in the Cyclades, Aegean Sea, Greece. *Geology*, 12, 221-225.
- Majer, V. and Mason, R., 1983. High pressure metamorphism between the Pelagonian Massif and Vardar Ophiolite belt, Yugoslavia. *Mineralogical Magazine*, 47, 139-141.
- Massonne, H.J., and Schreyer, W., 1987. Phengite geobarometry based on the limiting assemblage with K-feldspar, phlogopite and quartz. *Contributions to Mineralogy and Petrology*, 96, 212-224.
- Medwenitsch, W., 1956. Zur Geologie Vardarisch-Makedoniens (Jugoslawien), zum Problem der Pelagoniden. *Oestereichische Akademie der Wissenschaften, Sitzungsberichte der mathematisch naturwissenschaftlichen Klasse, Abteilung 1*, 165, 397-473.
- Mercier, J., 1968. Etude géologique des zones Hellénides en Macédoine centrale (Grece). *Annale Géologique de Pays Hellénique*, 20, 17-92.
- Mercier, J.P. Vergely and Bebieu, J., 1975. Les ophiolites helléniques "Obductées" au Jurassique supérieur sontelles les vestiges d' un ocean téthysien ou d' une ocean téthysien ou d'une mer marginale peri-europeenne? *Compte Rendue sommaire des Séances de la Société Géologique de France*, 17, 108-112.
- Migiros, A. and Galeos, A., 1990. Tectonic and stratigraphic significance of the Ano Garefi ophiolitic rocks Northern Greece). In: J. E. Malpas, E. Moores, A. Panayiotou and E. Xenophonos (eds), *Ophiolites: Oceanic Crustal Analogues. Proceedings Symposium Troodos 1987*, Geological Survey Department, Nicosia, pp. 279-284.
- Most, T., 2003. Geodynamic evolution of the Eastern Pelagonian zone in Northwestern Greece and the republic of Macedonia. PhD Thesis, University of Tuebingen, Tuebingen, 195 pp.
- Most, T., Frisch, W., Dunkl, I., Kadosa, B., Boev, B., Avgerinas A. and Kilias, A., 2001. Geochronological and structural investigation of the Northern Pelagonian crystalline zone. Constraints from K/Ar and zircon and apatite fission track dating. *Bulletin of Geological Society of Greece*, 34, 91-95.
- Mountrakis, D. 1986. The Pelagonian zone in Greece: A poly-phase deformed fragment of the Cimmerian continent and its role in the geotectonic evolution of the Eastern Mediterranean. *Journal of Geology*, 94, 335-347.
- Mposkos, E. Kostopoulos, D.K. and Krohe, A., 2001. LowP/HighT prealpine metamorphism and medium P alpine overprint of the Pelagonian zone documented in high-alumina metapelites from the Vernon massif, Western Macedonia, Northern Greece. *Bulletin of Geological Society of Greece*, 34, 949-958.
- Nance, D., 1981. Tectonic history of a segment of the Pelagonian zone, Northeastern Greece. *Canadian Journal of Earth Sciences*, 18, 1111-1126.
- Neubauer, F., Dallmeyer, R.D, Dunkl, I. and Schirnik, D., 1995. Late Cretaceous exhumation of the metamorphic Gleinalm dome, Eastern Alps: kinematics, cooling history and sedimentary response in a sinistral wrench corridor. *Tectonophysics*, 242, 79-98.
- Pamic, J., 2002. The SavaVardar zone of the Dinarides and Hellenides versus the Vardar Ocean. *Eclogae Geologicae Helveticae*, 95, 99-113.
- Pangea scientific, 2005. My Fault, Version 1,03.
- Papanikolaou D. 2009. Timing of tectonic emplacement of the ophiolites and terrane paleogeography in the Hellenides. *Lithos*, 108, 262-280.
- Pavlidis, S., Mountrakis, D., Kilias, A., and Tranos, M., 1990. The role of strikeslip movements in the extensional area of the northern Aegean Greece). *Annale Tectonique*, 4, 196-211.

- Platt, J.P., 1993. Exhumation of high –pressure rocks: a review of concepts and processes. *Terra Nova*, 5, 119-133.
- Platt, J.P., Soto, J.I., Whitehouse, M.J., Hurford, A.J., and Kelley, S.P., 1998. Thermal evolution, rate of exhumation, and tectonic significance of metamorphic rocks from the floor of the Alboran extensional basins, western Mediterranean. *Tectonics*, 17, 671-689.
- Rassios, A.H.E. and Moores, E.M., 2006. Heterogeneous mantle complex, crustal processes, and obduction kinematics in a unified Pinodos-Vourinos ophiolitic slab. In: A.H.F. Robertson and D. Mountrakis (eds), *Tectonic Development of the Eastern Mediterranean region*. Geological Society of London, Special Publication, 260, pp. 237-266.
- Rassios A.H.E. and Dilek Y., 2009. Rotational deformation in the Jurassic Mesohellenic ophiolites, Greece, and its tectonic significance. *Lithos*, 108, 207-223.
- Ratschbacher, L., Frisch, W., Neubauer, F., Schmid, S.M. and Neugebauer, J. 1989. Extension in compressional orogenic belts: The eastern Alps. *Geology*, 17, 404-407.
- Ricou, L.E., Burg, J.P., Godfriaux, I. and Ivanov, Z. 1998. Rhodope and Vardar: the metamorphic and the olistostromic paired belts related to the Cretaceous subduction under the Europe. *Geodynamica Acta*, 1998, 11,6, 285-309.
- Robertson, A.H.F. and Shallo, M., 2000. Mesozoic-Tertiary tectonic evolution of Albania in its regional Eastern Mediterranean context. *Tectonophysics*, 316, 197-214.
- Robertson, A.H.F., Dixon, J.E., Brown S. et al. 1996. Alternative tectonic models for the Late Palaeozoic – Early Tertiary development of Tethys in the Eastern Mediterranean. In: J.E. Dixon and A.H.F. Robertson (eds), *The Geological Evolution of the Eastern Mediterranean*. Geological Society of London Special Publications, 17, pp. 1-74.
- Roddick, J. Cameron, W., and Smith, A.G., 1979. Permo-Triassic and Jurassic Ar/Ar ages from Greek ophiolites and associated rocks. *Nature*, 279, 788-790.
- Schermer, R.E. 1993. Geometry and kinematics of continental basement deformation during the Alpine orogeny, Mt. Olympos region, Greece. *Journal of Structural Geology*, 15, 571-591.
- Schermer, R.E., Lux, D.R. and Burchfiel, B.C., 1990. Temperature-time history of subducted continental crust, Mt. Olympos region, Greece. *Tectonics*, 9, 1165-1195.
- Scherreiks, R., Bosence, D., BouDagher-Fadel, M., Malendez, G., Baumgartner, P.O., 2009. Evolution of the Pelagonian carbonate platform complex and the adjacent oceanic realm in response to plate tectonic forcing (Late Triassic and Jurassic), Evvoia, Greece. *International Journal of Earth Sciences* (in press).
- Schliestedt, M., Altherr, R., and Mattheus, A. 1987. Evolution of the Cycladic Crystalline complex: Petrology, isotope geochemistry and geochronology. In: H.C. Helgeson (ed), *Chemical Transport in Metasomatic Processes*. NATO ASI Series 218C, D. Reidel, Dordrecht, pp. 389-428.
- Schlagintweit, F., Gawlick, H.J., Missoni, S., Hoxha, L., Lein, R. and Frisch, W., 2008. The eroded Late Jurassic Kurbnesh carbonate platform in the Mirdita Ophiolite Zone and its bearing on the Jurassic orogeny of the Neotethys realm. *Swiss Journal Geosciences*, 101, 125-138.
- Schmid, S., Bernoulli, D., Fuegenschuh, B., Matenco L., Schefer, S., Schuster, R., Tischler, M. and Ustaszewski, K. 2008. The Alpine-Carpathian –Dinaric orogenic system: correlation and evolution of tectonic units. *Swiss Journal of Geosciences*, 101, 139-183.
- Schreurs, J., 1985. Prograde metamorphism of metapelites garnet-biotite thermometry and prograde changes of biotite chemistry, in high grade rocks of west Unsime, southwest Finland. *Lithos*, 18, 69-80.
- Seidel, E., Kreuzer, H. and Harre, W., 1982. A Late Oligocene/Early Miocene high pressure belt in the external Hellenides. *Geologisches Jahrbuch*, E 23, 165-206.
- Sfeikos, A. 1992. Analysis of deformation and kinematics of the Pelagonian nappe system. Kamvounia mountain North Thessaly, Greece). PhD Thesis, University of Tuebingen, Tuebingen, 160 pp.
- Sfeikos, A., Boehringer, Ch., Frisch, W., Kilias, A. and Ratschbacher, L., 1991. Kinematics of Pelagonian nappes in the Kranea area, North Thessaly, Greece. *Bulletin of Geological Society of Greece*, 25, 101-115.
- Shallo, M. and Dilek, Y., 2003. Development of the ideas on the origin of Albanian ophiolites. *Geological Society of America Bulletin*, Special Publication, 373, 351-363.
- Sharp, I.R. and Robertson, A.H.F., 2006. Tectonic-sedimentary evolution of the western margin of the Mesozoic Vardar Ocean: evidence from the Pelagonian and Almopias zones, northern Greece. In: A.H.F. Robertson and D. Mountrakis (eds), *Tectonic Development of the Eastern Mediterranean Region*. Geological Society of London, Special Publication, 260, pp. 373-412.
- Simpson, C. and Schmid, S.M., 1983. An evaluation of criteria to deduce the sense of movement in sheared rocks. *Geological Society of America Bulletin*, 94, 1281-1288.
- Smith, A.G. 2006. Tethyan ophiolite emplacement, Africa to Europe motions, and Atlantic spreading. In: A.H.F. Robertson and D. Mountrakis (eds), *Tectonic Development of the Eastern Mediterranean region*. Geological Society of London Special publications, 260, pp. 1-134.

- Spear, F.S., Hickmott, D.D., and Selverstone, J., 1990. Metamorphic consequences of thrust emplacement. Fall Mountains, New Hampshire. *Geological Society of America Bulletin*, 102, 1344-1360.
- Spray, J.G. and Roddick, J.C., 1980. Petrology and $^{40}\text{Ar}/^{39}\text{Ar}$ geochronology of some Hellenic subophiolitic metamorphic rocks. *Contributions to Mineralogy and Petrology*, 72, 43-55.
- Stampfli, G.M. and Borel, G.D., 2002. A plate tectonic model for the Palaeozoic and Mesozoic constrained by dynamic plate boundaries and restored synthetic oceanic isochrones. *Earth and Planetary Science Letters*, 169, 17-33.
- Vavassis, A., De-Bono, G.M., Stampfli, D., Giorgis, A., Valloton, A. and Amelin Y., 2000. U-Pb and Ar-Ar geochronological data from the Pelagonian basement in Evia (Greece) : geodynamic implications for the evolution of Paleotethys. *Schweizerische Mineralogische Petrologische Mitteilungen*, 80, 21-43.
- Vergely, P. 1984. Tectoniques des ophiolites dans les Hellénides Internes déformation, métamorphismes et phénomènes sédimentaires) Consequences sur l' évolution des régions Téthysiennes Occidentales. PhD Thesis, Université de Paris – Sud, Orsay, 560 pp.
- Vidal, O., Goffe, B., Bousquet, R., and Parra, T., 1999. Calibration and testing of an empirical chloritoid-chlorite Mg-Fe exchange thermometer and thermodynamic data for daphnite. *Journal of Metamorphic Geology*, 17, 25-39.
- Wu, C.M., Wang, X. S., Yang, C. H., Geng Y.S. and Liu, F.I., 2002. Empirical garnet-muscovite geothermometry in metapelites. *Lithos*, 62, 113.
- Xie, X., Byerly, R., and Ferrelli, E., 1997. Ilb ti octahedral chlorite from the Barberton greenstone belt: crystal structure and rock composition constraints with implications to geothermometry. *Contributions to Mineralogy and Petrology*, 126, 275-291.
- Xypolias, P., Kokkalas, S., and Skourlis, K., 2003. Upward extrusion and subsequent transpression as a possible mechanism for the exhumation of HP/LT rocks in Evia Island (Aegean Sea, Greece). *Journal of Geodynamics*, 35, 303-320.
- Yarwood, G.A. and Aftalion M., 1976. Field relations and U-Pb geochronology of a granite from the Pelagonian Zone of the Hellenides (High Pieria, Greece). *Bulletin de la Société Géologique France*, 18/2, 259-264.
- Yarwood, G.A. and Dixon, J.E., 1977. Lower Cretaceous and younger thrusting in the Pelagonian rocks of the High Pieria, Greece. In: Kallergis (ed). *Proceedings of the 6th colloquium on the geology of the Aegean region*, Athens, pp. 269-280.
- Zang, W. and Fyfe, W.S., 1995. Chloritisation of the hydrothermally altered bedrock at the Igarape Bahia gold deposit, Brazil. *Mineralium Deposita*, 30, 30-38.
- Zimmerman, J.Jr. and Ross, J.V., 1976. Structural evolution of the Vardar root zone, northern Greece: Discussion and reply. *Bulletin of Geological Society of America*, 90, 126-128.

Received: 23. February 2009

Accepted: 2. February 2010

Adamantios KILIAS^{1*)}, Wolfgang FRISCH²⁾, Asterios AVGERINAS¹⁾, Istvan DUNKL³⁾, George FALALAKIS¹⁾ & Hans-Jürgen GAWLICK⁴⁾

¹⁾ Department of Geology and Paleontology, University of Thessaloniki, GR-54124, Thessaloniki, Greece;

²⁾ Institute of Geosciences, University of Tuebingen, D-72076, Tuebingen, Germany;

³⁾ Sedimentology and Environmental Geology Geoscience center, University of Goettingen, D-37077, Goettingen, Germany;

⁴⁾ Department for Applied Geosciences and Geophysics, University of Leoben, A-8700, Leoben, Austria;

* Corresponding author, kilias@geo.auth.gr